Electronic Supplementary Material (ESI) for New Journal of Chemistry.

A simple D–π–A system of phenanthroimidazole-π-fluorenone for highly efficient non-doped bipolar AIE luminogens: Synthesis, molecular optical, thermal and electrochemical properties

Devarajan Kathirvelan[a], Sivakalai Mayakrishnan[b], Narayanan Uma Maheswari[b], Chinmoy Biswas[c], Sai Santosh Kumar Raavi[c], Tarun K Panda[a*]

** Corresponding author*

[a] Department of Chemistry, Indian Institute of Technology Hyderabad, Kandi, Sangareddy 502285, India.

[b] Organic & Bioorganic Chemistry Laboratory, CSIR-Central Leather Research Institute, Chennai 600 020, India.

[c] Department of Physics, Indian Institute of Technology Hyderabad, Kandi, Sangareddy -502 285, India.

Supporting Information

Contents

1. Materials and Methods

All the chemicals were purchased from commercial sources especially from Sigma Aldrich and used without any further purification. The synthetic strategy to obtain the targeted PI fluorophores was carried out by condensation reaction product reacted with relevant boronic acid by Suzuki coupling reaction. The synthetic strategy to obtain the target PI fluorophores has been provided in Scheme. The compound characterized for ^{1} H NMR, ^{13}C NMR and DEPT spectra were performed 400 MHz and 100 MHz Bruker spectrometer. The Chemical shifts values in parts per million (ppm) with TMS (0 ppm) and $CDCl_3$-DMSO-D_6 as standards for ^{1}H NMR and ^{13}C NMR spectra. Infrared spectroscopy of all the compound were measured using Bruker- Alpha-p instrument. All the TLC analyses were carried out using Merck silica gel 60 F254 plates. UV-vis absorption spectra of all compounds were recorded in DMSO on a Bruker UV–visible spectrophotometer. Emission spectra were taken in a Bruker fluorescence spectrophotometer. The excitation and emission slits were 3 nm wide for the emission measurements. All the measurements were done at 298 K. Column chromatography was performed on Merck silica gel (100–200 mesh).

2. Synthesis of Precursors:

2.1 Experimental procedures for the Synthesis of 2-(4-bromophenyl)-1-phenyl-1H-phenanthro[9,10-d]imidazole (S-1)

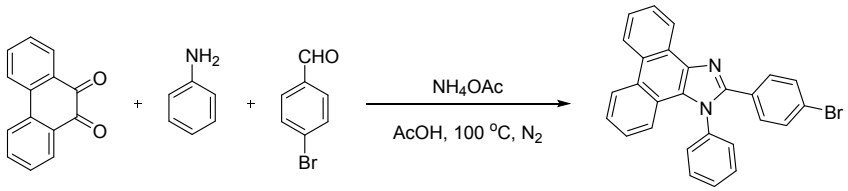

S-1

Compound S-1 was prepared by refluxing of 9,10-phenanthrenequinone 1.00 g (1.0 equiv), 4-bromo benzaldehyde 0.977 g (1.10 equiv), Aniline 0.893 g (2.00 equiv) and ammonium acetate 1.109 g (3.00 equiv) in glacial acetic acid 50 ml. The reaction mixture was heated at 120 °C for 24 h under an nitrogen atmosphere. After cooling to room temperature, the dark-yellow mixture was poured into a methanol solution with stirring. The separated solid was filtered off, washed with cold methanol and dried to give a S-1 white solid yield of 80%.

2.2 Synthesis of 2-(4-bromophenyl)-1-(4-methoxyphenyl)-1H-phenanthro[9,10-d]imidazole (S-2)

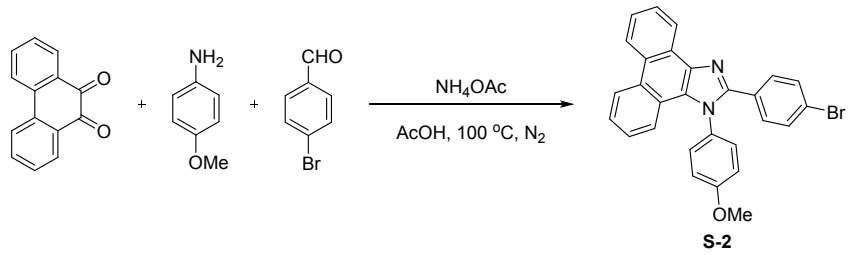

S-2

Compound S-2 was prepared by refluxing of 9,10-phenanthrenequinone 1.00 g (1.0 equiv), 4-bromo benzaldehyde 0.977 g (1.10 equiv), 4-methoxyaniline 1.18 g (2.00 equiv) and ammonium acetate 1.109 g (3.00 equiv) in glacial acetic acid 50 ml. The reaction mixture was heated at 120 °C for 24 h under a nitrogen atmosphere. After cooling to room temperature, the dark-yellow mixture was poured into a methanol solution with stirring. The separated solid was filtered off, washed with cold methanol and dried to give a S-2 white solid yield of (72%).

2.3 Synthesis of 4-(2-(4-bromophenyl)-1H-phenanthro[9,10-d]imidazol-1-yl)benzonitrile (S-3)

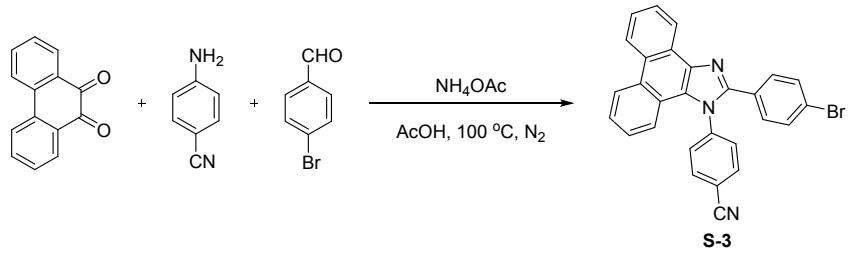

S-3

Compound S-3 was prepared by refluxing of 9,10-phenanthrenequinone 1.00 g (1.0 equiv), 4-bromo benzaldehyde 0.977 g (1.10 equiv), 4-aminobenzonitrile 1.13 g (2.00 equiv) and ammonium acetate 1.109 g (3.00 equiv) in glacial acetic acid 50 ml. The reaction mixture was heated at 120 °C for 24 h under an nitrogen atmosphere. After cooling to room temperature, the dark-yellow mixture was poured into a methanol solution with stirring. The separated solid was filtered off, washed with cold methanol and dried to give a S-3 white solid yield of (86%).

2.4 Synthesis of 2-(6-bromonaphthalen-2-yl)-1-phenyl-1H-phenanthro[9,10-d]imidazole (S-4)

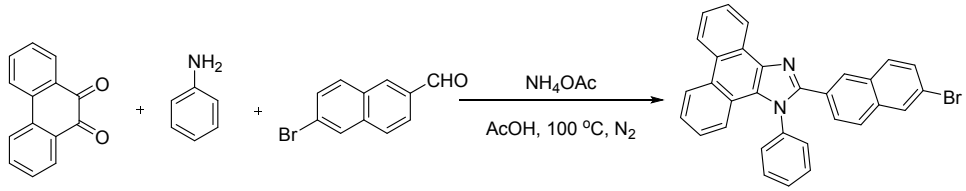

S-4

Compound S-4 was prepared by refluxing of 9,10-phenanthrenequinone 1.00 g (1.0 equiv), 6-bromo-2-naphthaldehyde 1.2 g (1.10 equiv), Aniline 0.890 g (2.00 equiv) and ammonium acetate 1.109 g (3.00 equiv) in glacial acetic acid 50 ml. The reaction mixture was heated at 120 °C for 24 h under an nitrogen atmosphere. After cooling to room temperature, the dark-yellow mixture was poured into a methanol solution with stirring. The separated solid was filtered off, washed with cold methanol and dried to give a S-4 white solid yield of (82%).

2.5 Synthesis of 2-(4-bromophenyl)-1-(4-butylphenyl)-1H-phenanthro[9,10-d]imidazole (S-5)

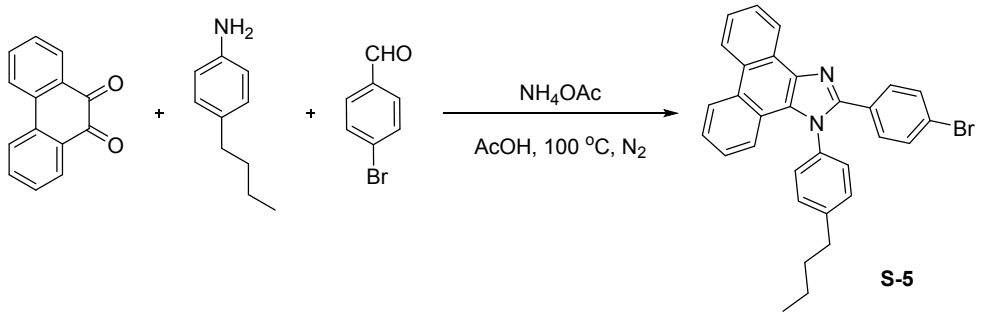

S-5

Compound S-5 was prepared by refluxing of 9,10-phenanthrenequinone 1.00 g (1.0 equiv), 6-bromo-2-naphthaldehyde 1.2 g (1.10 equiv), 4-butyl aniline 1.43 g (2.00 equiv) and ammonium acetate 1.109 g (3.00 equiv) in glacial acetic acid 50 ml. The reaction mixture was heated at 120 °C for 24 h under an nitrogen atmosphere. After cooling to room temperature, the dark-yellow mixture was poured into a methanol solution with stirring. The separated solid was filtered off, washed with cold methanol and dried to give a S-5 white solid yield of (82%).

3. Synthesis of Final Products (P1-P5)

3.1 Procedure for the synthesis of P1-5 using Suzuki coupling reaction

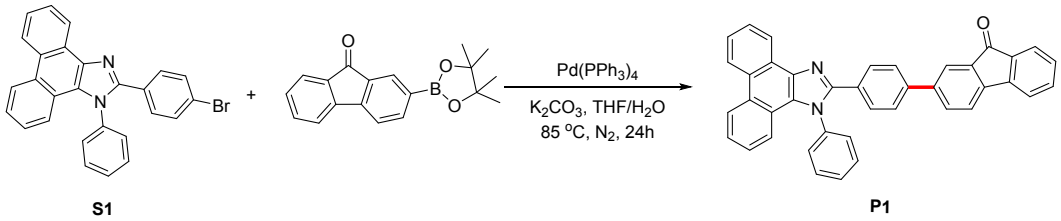

S1 P1

To an oven-dried 50 mL double neck round bottom flask fitted with a reflux condenser were added 2-(4-bromophenyl)-1-phenyl-1H-phenanthro[9,10-d]imidazole S-1 269 mg (0.6 mmol, 1.00 equiv), 2-(4,4,5,5-tetramethyl-1,3,2-dioxaborolan-2-yl)-9H-fluoren-9-one 183 mg (0.6 mmol, 1.00 equiv), $Pd(PPh_3)_4$ 69 mg (10.0 mol %) and K_2CO_3 165 mg (2.0 equiv) in THF/H_2O (7:3). The reaction mixture was heated and refluxed at 85 °C for 24 h. After cooling to ambient temperature, the reaction mixture was diluted with MDC, filtered through celite and the filtrate was concentrated under reduced pressure. The crude residue was purified through a silica gel column using hexane and MDC as eluent to provided desired product **P-1** in 70 % of yield yellow solid.

3.2 Synthesis of 2-(4-(1-(4-methoxyphenyl)-1H-phenanthro[9,10-d]imidazol-2-yl)phenyl)-9H-fluoren-9-one(P-2)

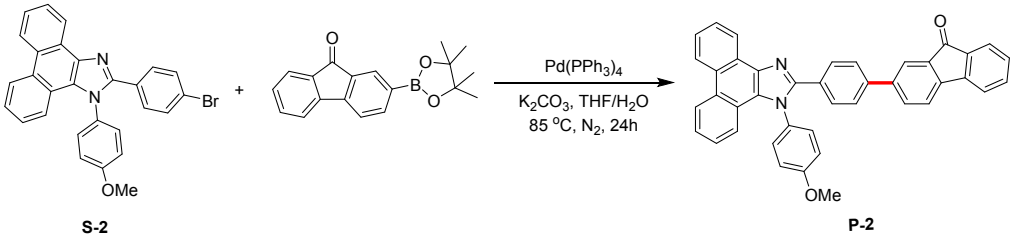

S-2 P-2

To an oven-dried 50 mL double neck round bottom flask fitted with a reflux condenser were added 2-(4-bromophenyl)-1-(4-methoxyphenyl)-1H-phenanthro[9,10-d]imidazole S-2 289 mg (0.6 mmol, 1.00 equiv), 2-(4,4,5,5-tetramethyl-1,3,2-dioxaborolan-2-yl)-9H-fluoren-9-one 183 mg (0.6 mmol, 1.00 equiv), $Pd(PPh_3)_4$ 69 mg (10.0 mol %) and K_2CO_3 166 mg (2.0 equiv) in THF/H_2O (7:3). The reaction mixture was heated and refluxed at 85 °C for 24 h. After cooling to ambient temperature, the reaction mixture was diluted with DCM, filtered through celite and the filtrate was concentrated under reduced pressure. The crude residue was purified through a silica gel (100-200 mesh) column using hexane and DCM as eluent to provided desired product **P-2** in 78 % of yield yellow solid.

3.3 Synthesis of 4-(2-(4-(9-oxo-9H-fluoren-2-yl)phenyl)-1H-phenanthro[9,10-d]imidazol-1-yl)benzonitrile (P-3)

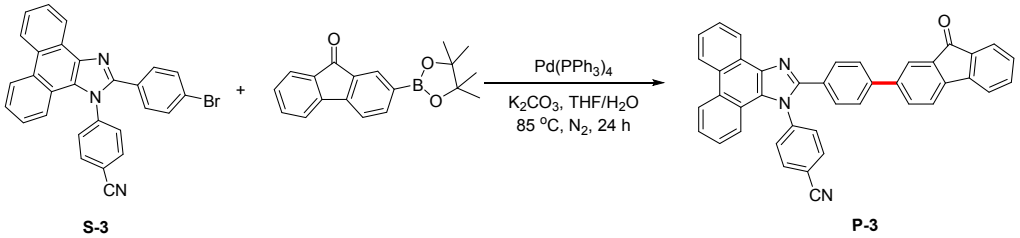

To an oven-dried 50 mL double neck round bottom flask fitted with a reflux condenser were added 4-(2-(4-bromophenyl)-1H-phenanthro[9,10-d]imidazol-1-yl)benzonitrile S-3 284 mg (0.6 mmol, 1.00 equiv), 2-(4,4,5,5-tetramethyl-1,3,2-dioxaborolan-2-yl)-9H-fluoren-9-one 183 mg (0.6 mmol, 1.00 equiv), $Pd(PPh_3)_4$ 69 mg (10.0 mol %) and K_2CO_3 165 mg (2.0 equiv) in THF/H_2O (7:3). The reaction mixture was heated and refluxed at 85 °C for 24 h. After cooling to ambient temperature, the reaction mixture was diluted with DCM, filtered through celite and the filtrate was concentrated under reduced pressure. The crude residue was purified through a silica gel column using hexane and DCM as eluent to provided desired product **P-3** in 62 % of yield yellow solid.

3.4 Synthesis of 2-(6-(1-phenyl-1H-phenanthro[9,10-d]imidazol-2-yl)naphthalen-2-yl)-9H-fluoren-9-one (P-4)

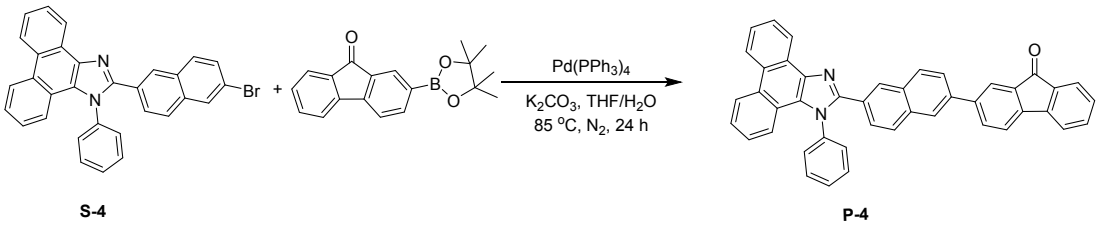

To an oven-dried 50 mL double neck round bottom flask fitted with a reflux condenser were added 2-(7-bromonaphthalen-2-yl)-1-phenyl-1H-phenanthro[9,10-d]imidazole S-4 299 mg (0.6 mmol, 1.00 equiv), 2-(4,4,5,5-tetramethyl-1,3,2-dioxaborolan-2-yl)-9H-fluoren-9-one 183 mg (0.6 mmol, 1.00 equiv), $Pd(PPh_3)_4$ 69 mg (10.0 mol %) and K_2CO_3 165 mg (2.0 equiv) in THF/H_2O (7:3). The reaction mixture was heated and refluxed at 85 °C for 24 h. After cooling to ambient temperature, the reaction mixture was diluted with DCM, filtered through celite and the filtrate was concentrated under reduced pressure. The crude residue was purified through a silica gel column using hexane and DCM as eluent to provided desired product **P-4** in 77 % of yield yellow solid.

3.5 2-(4-(1-(4-butylphenyl)-1H-phenanthro[9,10-d]imidazol-2-yl)phenyl)-9H-fluoren-9-one (P-5)

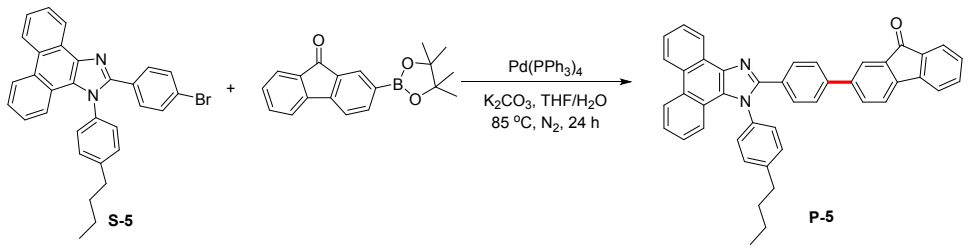

To an oven-dried 50 mL double neck round bottom flask fitted with a reflux condenser were added 2-(4-bromophenyl)-1-(4-butylphenyl)-1H-phenanthro[9,10-d]imidazole S-5 303 mg (0.6 mmol, 1.00 equiv), 2-(4,4,5,5-tetramethyl-1,3,2-dioxaborolan-2-yl)-9H-fluoren-9-one 183 mg (0.6 mmol, 1.00 equiv), $Pd(PPh_3)_4$ 69 mg (10.0 mol %) and K_2CO_3 165 mg (2.0 equiv) in THF/H_2O (7:3). The reaction mixture was heated and refluxed at 85 °C for 24 h. After cooling to ambient temperature, the reaction mixture was diluted with DCM, filtered through celite and the filtrate was concentrated under reduced pressure. The crude residue was purified through a silica gel column using hexane and DCM as eluent to provided desired product **P-5** in 85 % of yield yellow solid.

4. Spectral Data for synthesized compounds (S1-S5)

2-(4-bromophenyl)-1-phenyl-1H-phenanthro[9,10-d]imidazole (S-1)

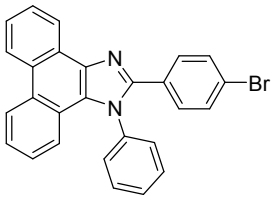

S-1

White solid; yield 80 %; **^{1}H NMR (400 MHz, DMSO-d_6)** δ 8.93 (d, *J* = 8.4 Hz, 1H), 8.88 (d, *J* = 8.3 Hz, 1H), 8.68 (d, *J* = 7.9 Hz, 1H), 7.78 (t, *J* = 7.5 Hz, 1H), 7.75 – 7.66 (m, 6H), 7.57 (t, *J* = 7.9 Hz, 3H), 7.51 (d, *J* = 8.6 Hz, 2H), 7.34 (t, *J* = 7.7 Hz, 1H), 7.08 (d, *J* = 8.3 Hz, 1H) ppm; **^{13}C NMR (100 MHz, DMSO-d_6)** δ 163.7, 161.6, 149.9, 138.4, 131.7, 131.4, 130.9, 129.9, 129.5, 129.0, 128.4, 128.2, 128.0, 127.1, 127.1, 126.3, 125.8, 125.0, 124.3, 124.1, 123.1, 122.8, 122.4, 120.6, 115.4 ppm.

2-(4-bromophenyl)-1-(4-methoxyphenyl)-1H-phenanthro[9,10-d]imidazole (S-2)

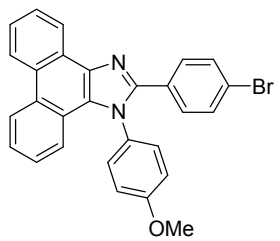

S-2

White solid; yield 72 %; **^{1}H NMR (400 MHz, DMSO-d_6)** δ 8.93 (d, *J* = 8.4 Hz, 1H), 8.88 (d, *J* = 8.3 Hz, 1H), 8.68 (d, *J* = 7.9 Hz, 1H), 7.77 (t, *J* = 7.4 Hz, 1H), 7.68 (t, *J* = 7.6 Hz, 1H), 7.65 – 7.50 (m, 7H), 7.39 (t, *J* = 7.6 Hz, 1H), 7.19 (dd, *J* = 14.1, 8.5 Hz, 3H),

3.90 (s, 3H) ppm; **^{13}C NMR (100 MHz, DMSO-d_6)** δ 160.5, 150.1, 136.8, 131.7, 131.4, 130.8, 130.6, 130.0, 129.01, 128.5, 128.1, 127.9, 127.2, 127.1, 126.2, 125.7, 124.9, 124.1, 123.1, 123.0, 122.4, 120.7, 115.9, 56.0 ppm.

4-(2-(4-bromophenyl)-1H-phenanthro[9,10-d]imidazol-1-yl)benzonitrile (S-3)

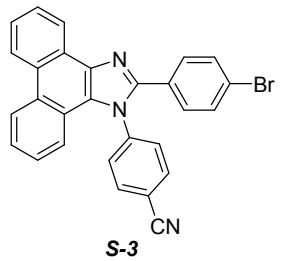

S-3

White solid; yield 86 %; **^{1}H NMR (400 MHz, DMSO-d_6)** δ 8.95 (d, *J* = 8.4 Hz, 1H), 8.89 (d, *J* = 8.3 Hz, 1H), 8.68 (d, *J* = 7.8 Hz, 1H), 8.19 (d, *J* = 8.3 Hz, 2H), 8.00 (d, *J* = 8.4 Hz, 2H), 7.78 (d, *J* = 7.7 Hz, 1H), 7.70 (t, *J* = 7.7 Hz, 1H), 7.59 (t, *J* = 8.4 Hz, 3H), 7.49 – 7.37 (m, 3H), 7.06 (d, *J* = 8.3 Hz, 1H) ppm; **^{13}C NMR (100 MHz, DMSO-d_6)** δ 149.9, 142.4, 137.2, 134.9, 131.8, 131.7, 130.9, 129.5, 129.1, 128.2, 128.2, 128.0, 127.4, 126.9, 126.4, 126.0, 125.1, 124.2, 123.4, 122.5, 122.5, 120.7, 118.5, 113.6 ppm.

2-(6-bromonaphthalen-2-yl)-1-phenyl-1H-phenanthro[9,10-d]imidazole (S-4)

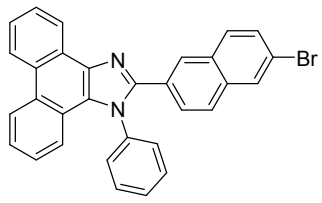

S-4

White solid; yield 82 %; **^{1}H NMR (400 MHz, DMSO-d_6)** δ 8.95 (d, *J* = 8.7 Hz, 1H), 8.90 (d, *J* = 8.3 Hz, 1H), 8.73 (d, *J* = 7.9 Hz, 1H), 8.21 (s, 1H), 8.09 (s, 1H), 7.88 (d, *J* = 8.4 Hz, 1H), 7.84 – 7.64 (m, 9H), 7.57 (d, *J* = 7.8 Hz, 1H), 7.36 (t, *J* = 7.7 Hz, 1H), 7.15 (d, *J* = 8.3 Hz, 1H) ppm; **^{13}C NMR (100 MHz, DMSO-d_6)** δ 144.99, 142.35, 141.14, 140.64, 139.98, 139.13, 138.14, 137.40, 136.46, 134.11, 132.97, 131.26, 130.90, 129.23, 129.15, 128.31, 127.98, 127.76, 127.43, 127.36, 127.24, 126.23, 123.78, 123.40, 123.01, 120.70, 119.38, 116.80 ppm.

2-(4-bromophenyl)-1-(4-butylphenyl)-1H-phenanthro[9,10-d]imidazole (S-5)

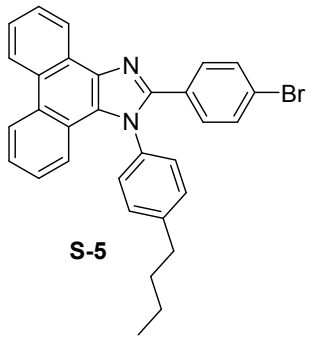

S-5

White solid; yield --%; **^{1}H NMR (400 MHz, $CDCl_3$)** δ 8.84 (dd, J = 8.0, 1.1 Hz, 1H), 8.75 (d, J = 8.3 Hz, 1H), 8.69 (d, J = 8.3 Hz, 1H), 7.73 (ddd, J = 8.0, 7.0, 1.1 Hz, 1H), 7.64 (ddd, J = 8.4, 7.0, 1.5 Hz, 1H), 7.53 – 7.35 (m, 9H), 7.28 – 7.23 (m, 1H), 7.19 (dd, J = 8.4, 1.4 Hz, 1H), 2.84 – 2.76 (m, 2H), 1.78 – 1.69 (m, 2H), 1.44 (dq, J = 14.6, 7.3 Hz, 2H), 1.01 (t, J = 7.4 Hz, 3H) ppm; **^{13}C NMR (100 MHz, $CDCl_3$)** δ 149.88, 145.25, 137.52, 136.14, 131.51, 130.91, 130.36, 129.74, 129.48, 128.82, 128.53, 128.44, 127.44, 127.31, 126.39, 125.80, 125.10, 124.23, 123.39, 123.26, 123.18, 122.81, 121.04, 35.53, 33.46, 22.40, 14.13 ppm;

5. Copies of NMR spectrum of synthesized compounds (S1-S5)

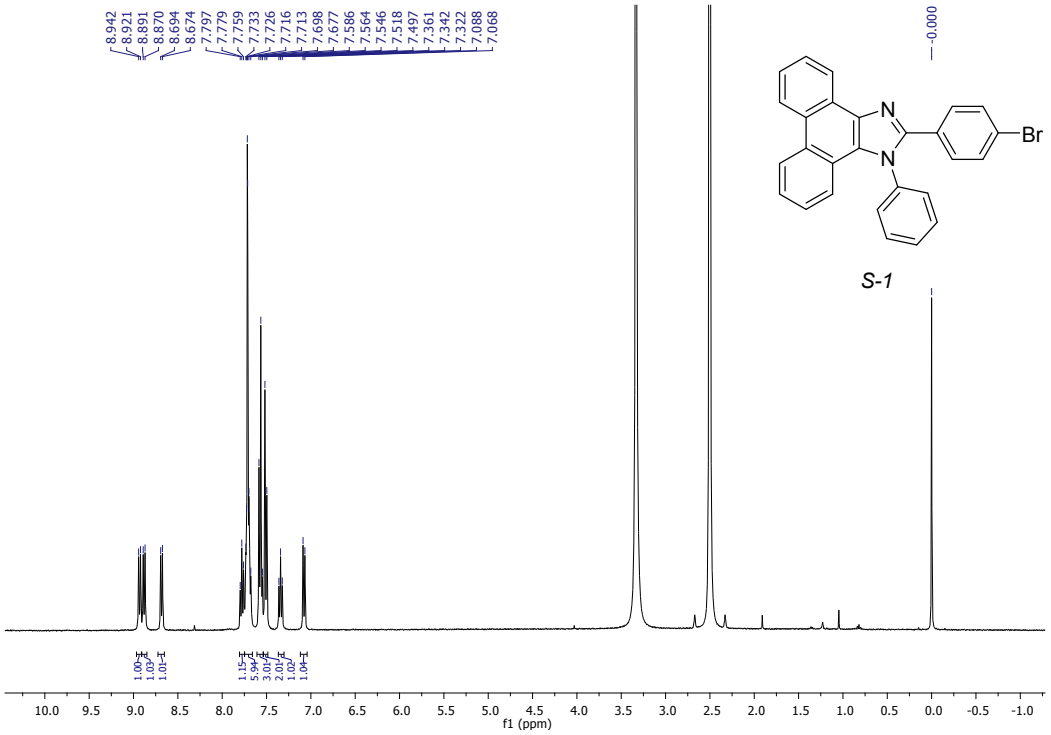

Figure S1:[1]H NMR spectrum of synthesised compound **S-1** in DMSO-d_6.

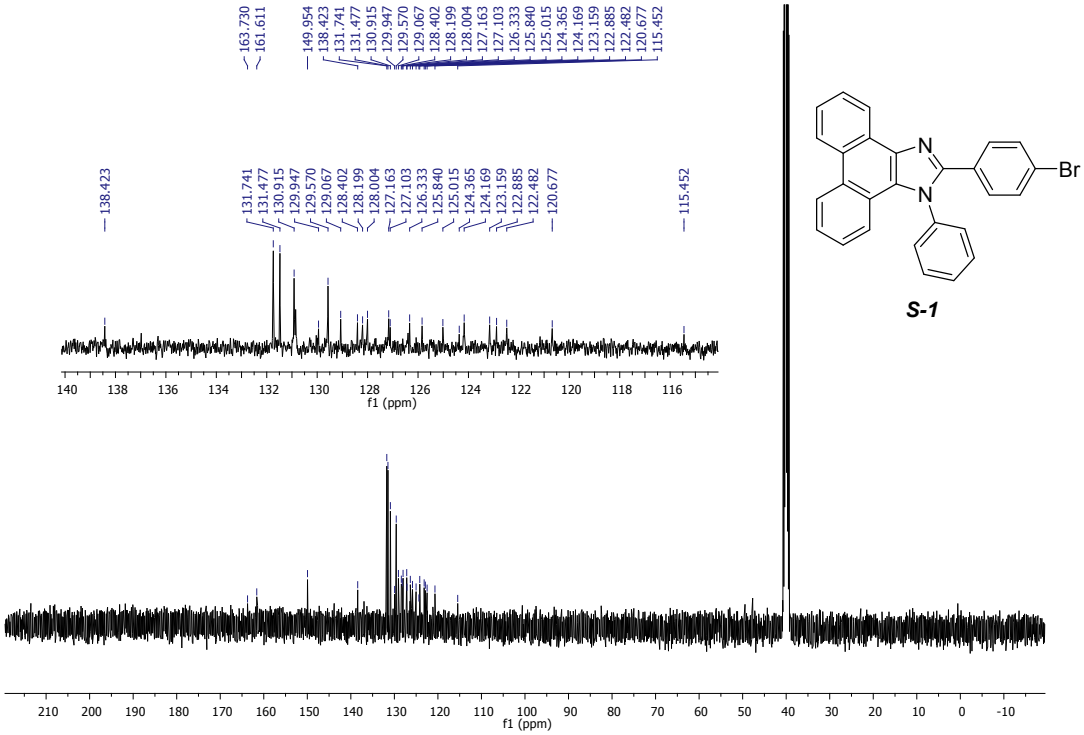

Figure S2:[13]C NMR spectrum of synthesised compound-**S1** in DMSO-d_6.

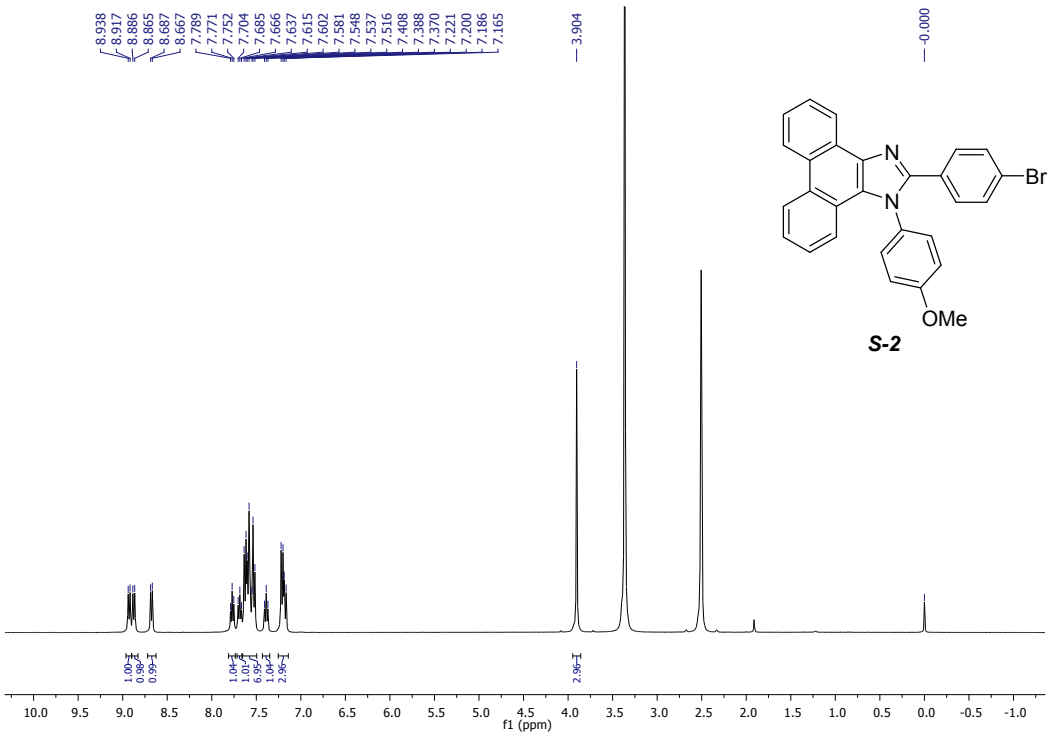

Figure S3:[1]H NMR spectrum of synthesised compound **S-2** in DMSO-d_6.

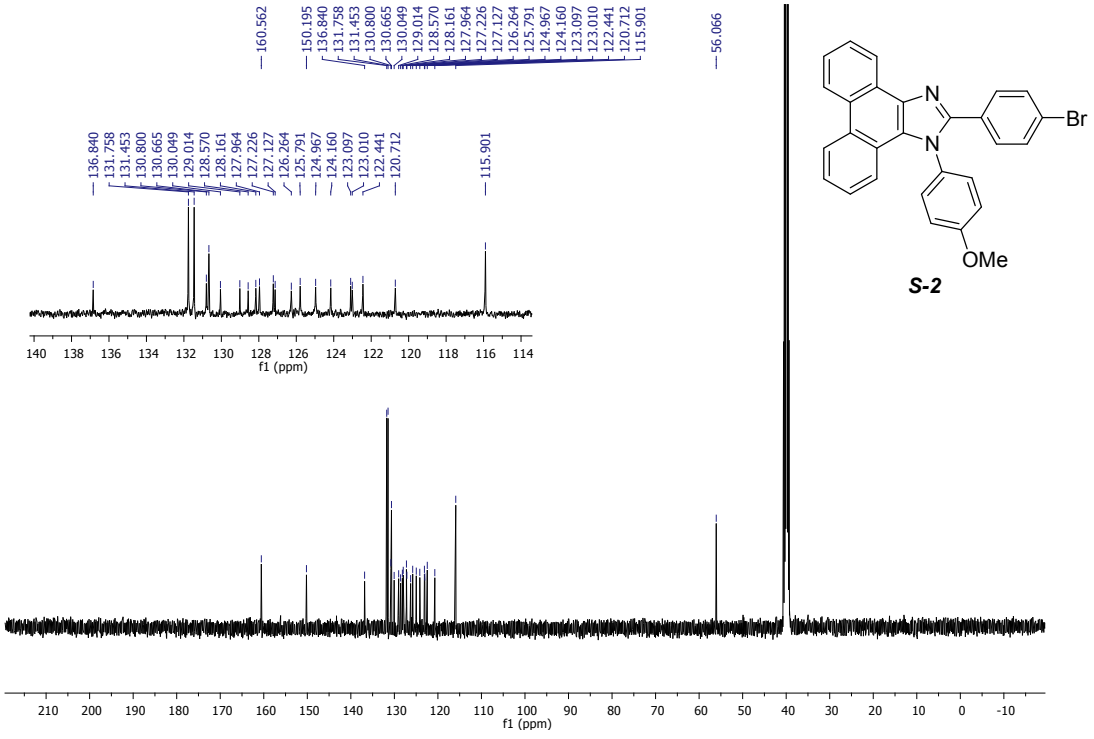

Figure S4:[13]C NMR spectrum of synthesised compound **S-2** in DMSO-d_6.

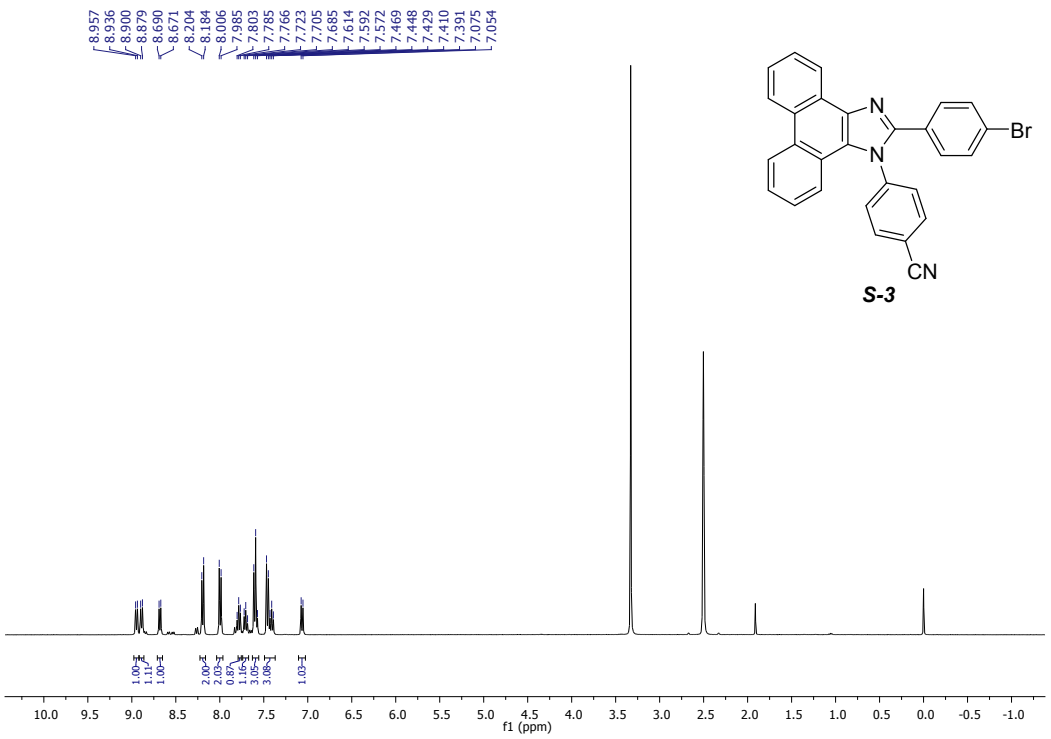

Figure S5:[1]H NMR spectrum of synthesised compound **S-2** in DMSO-d_6.

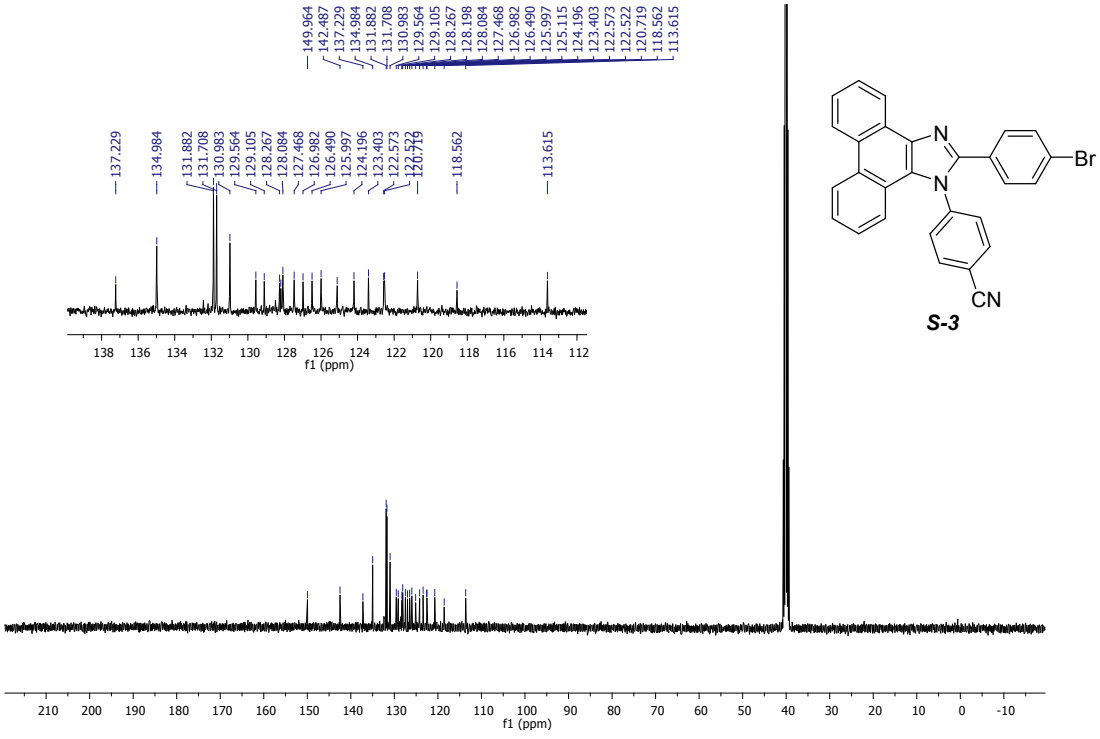

Figure S6:[13]C NMR spectrum of synthesised compound **S-2** in DMSO-d_6.

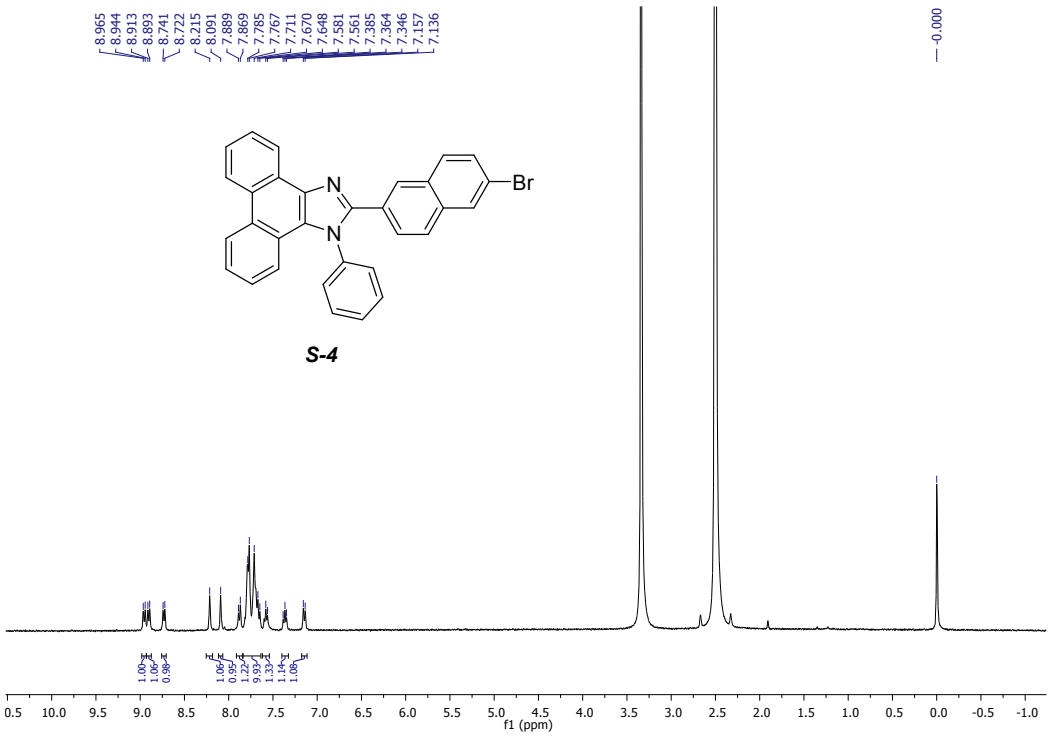

Figure S7:[1]H NMR spectrum of synthesised compound **S-4** in DMSO-d_6.

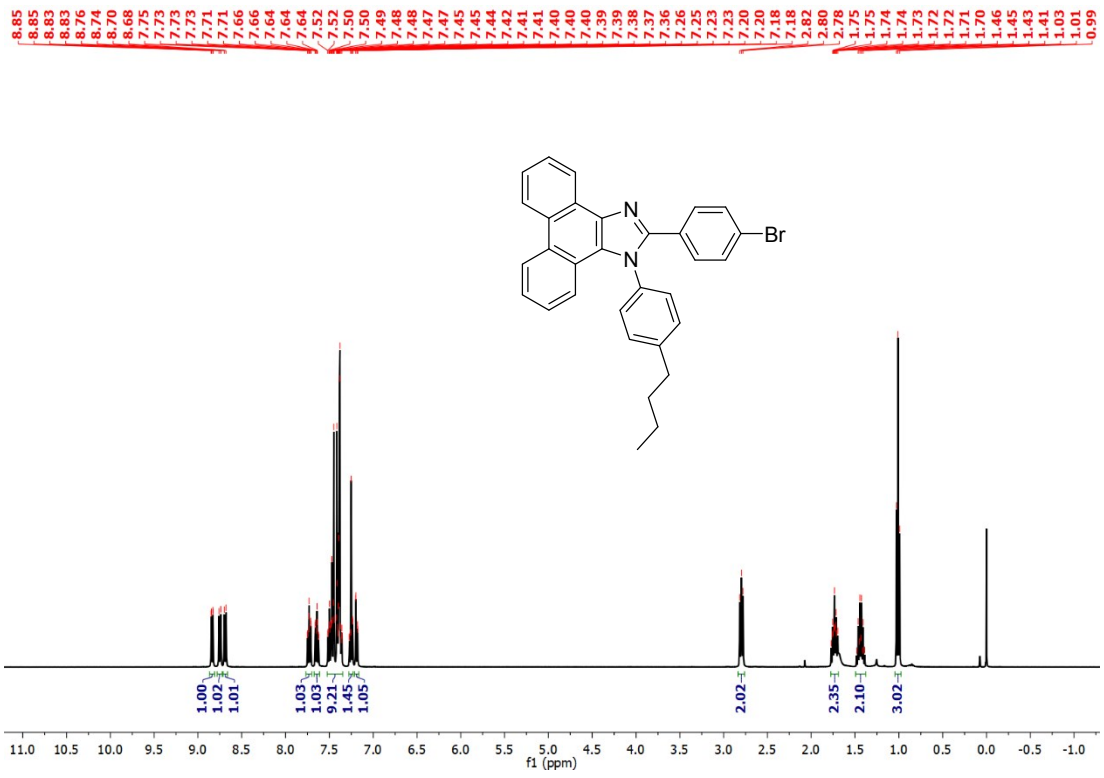

Figure S8:[1]H NMR spectrum of compound **S-5** in $CDCl_3$.

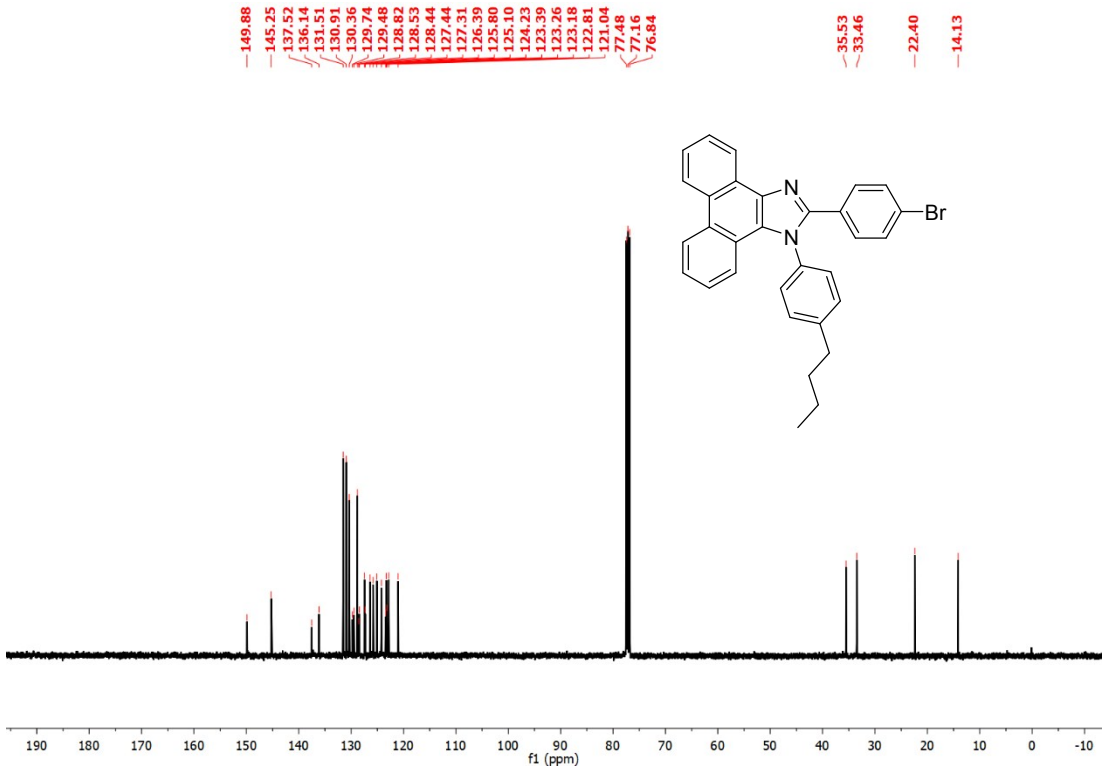

Figure S9:^{13}C NMR spectrum of compound **S-5** in $CDCl_3$.

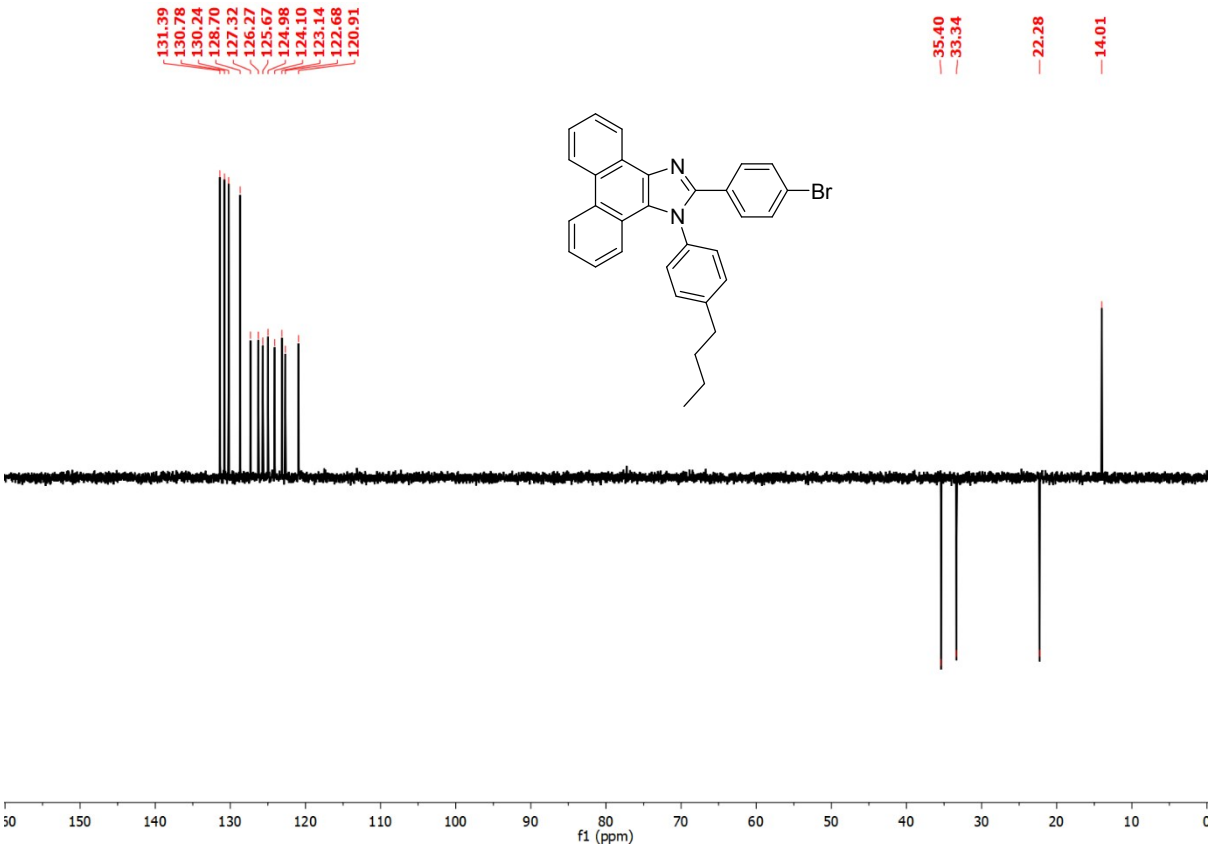

Figure S10: Dept-135 NMR spectrum of compound **S-5** in $CDCl_3$.

6. Copies of ^{1}H, ^{13}C NMR and Mass spectrum of synthesized compounds (P1-P5)

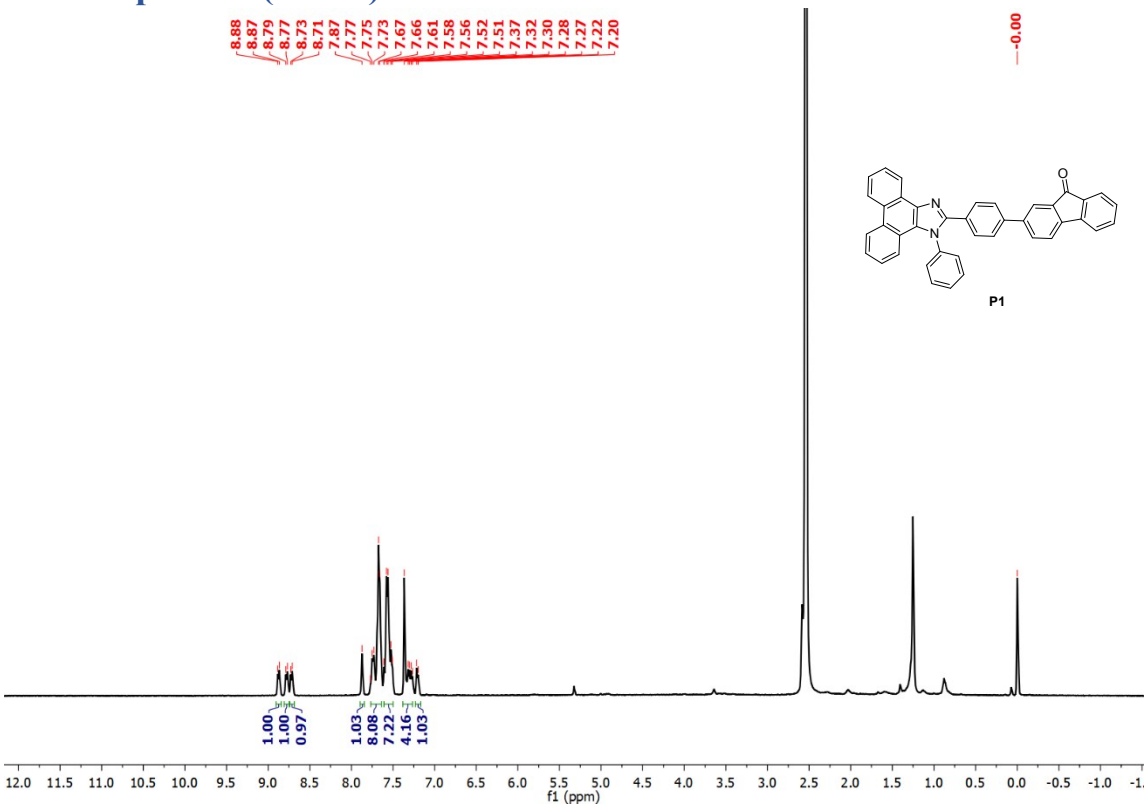

Figure S11:^{1}H NMR Spectrum of compound **P-1** in $CDCl_3$+DMSO-d_6.

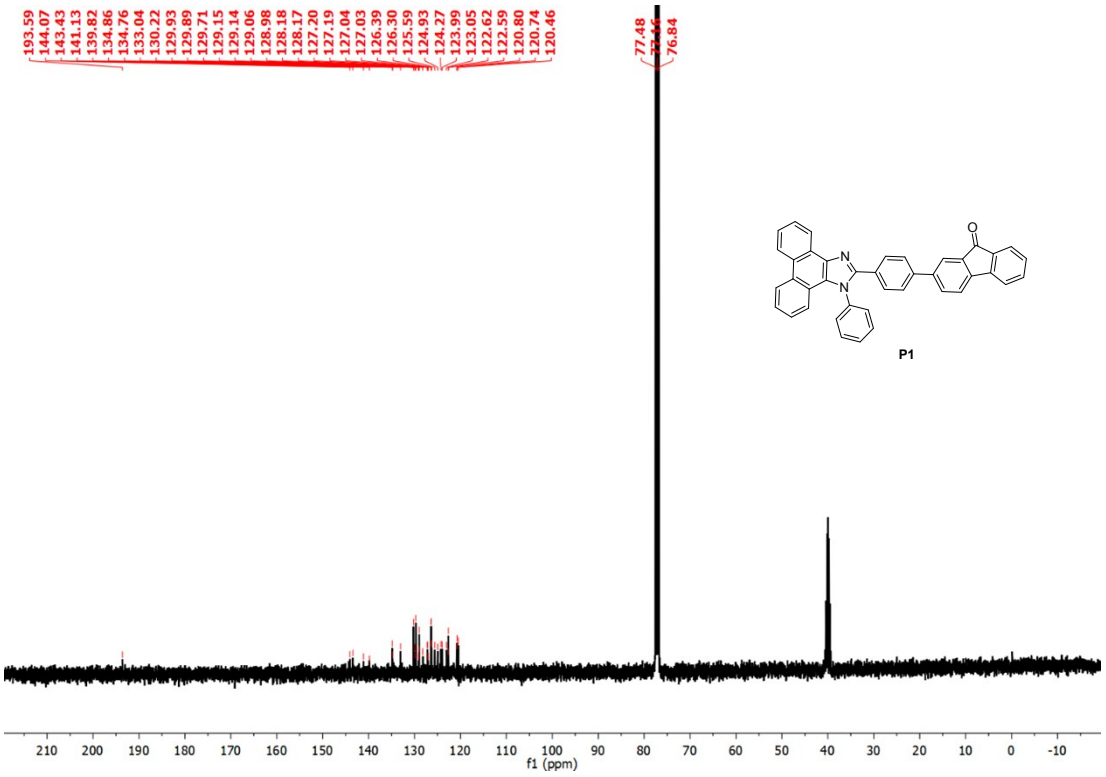

Figure S12:^{13}C NMR Spectrum of compound **P-1** in $CDCl_3$+DMSO-d_6.

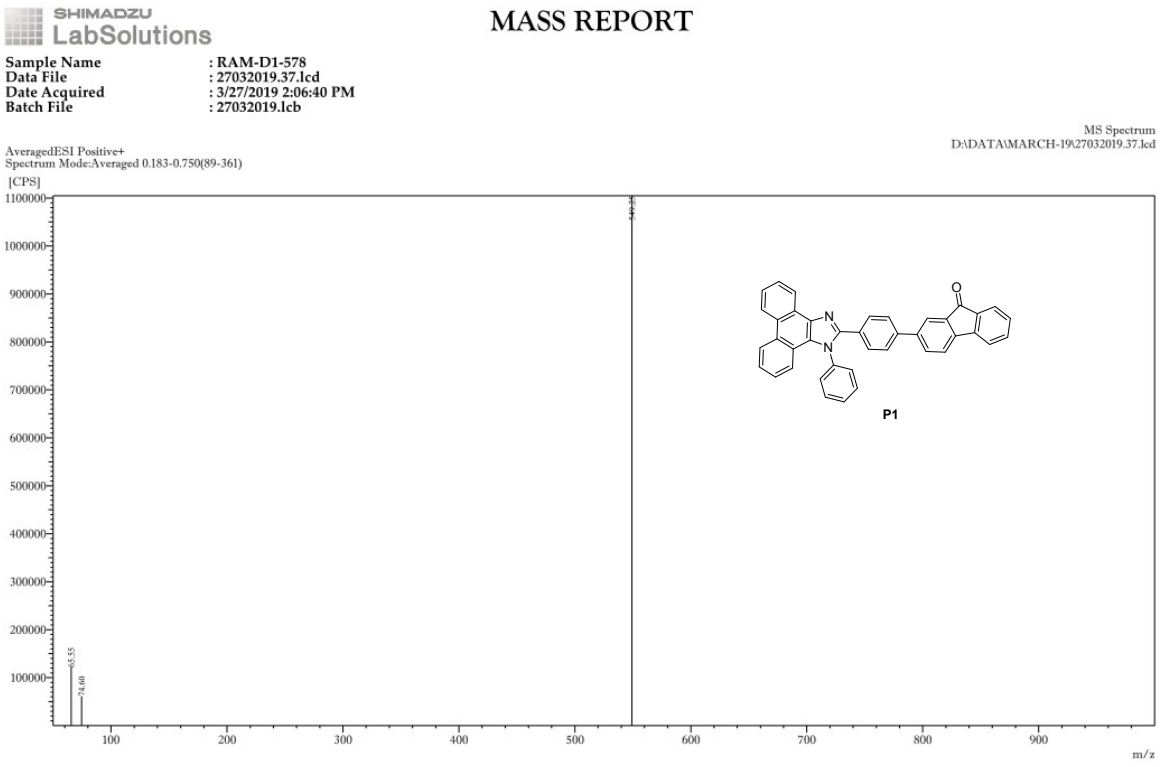

Figure S22: ESI MASS spectra of the luminogen **P-1**.

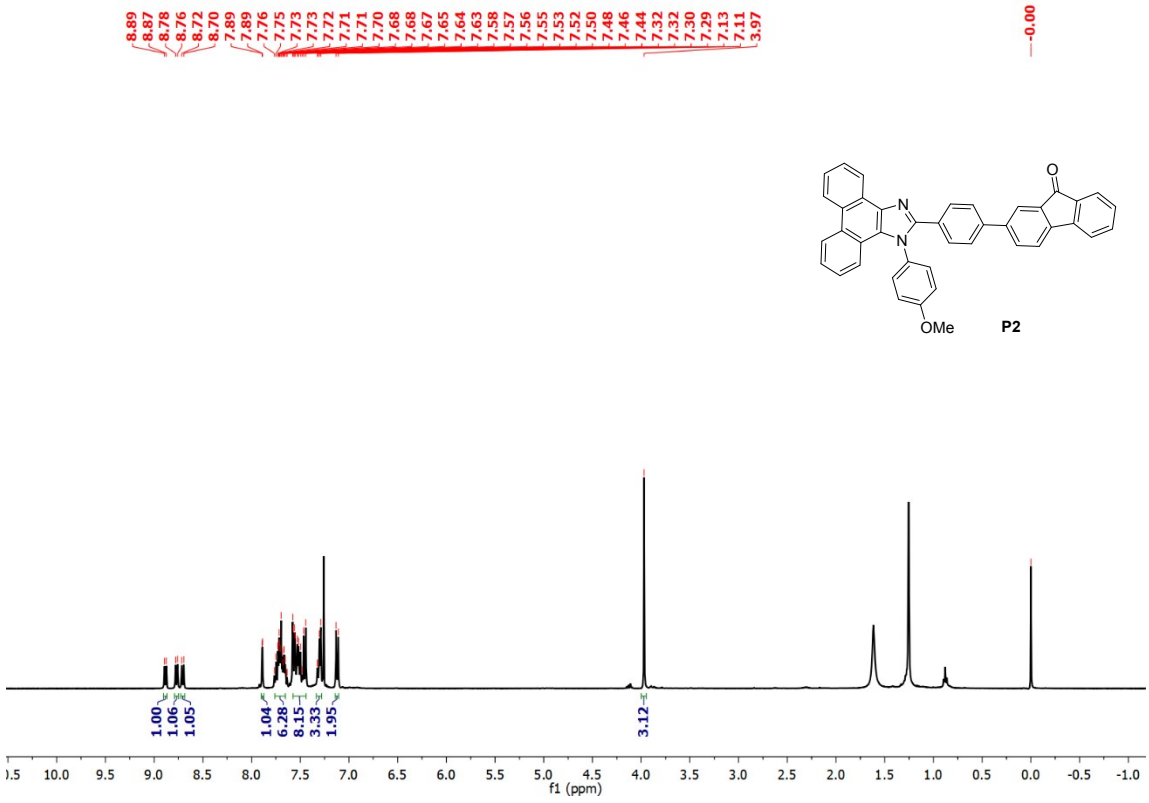

Figure S13:^{1}H NMR Spectrum of compound **P-2** in $CDCl_3$.

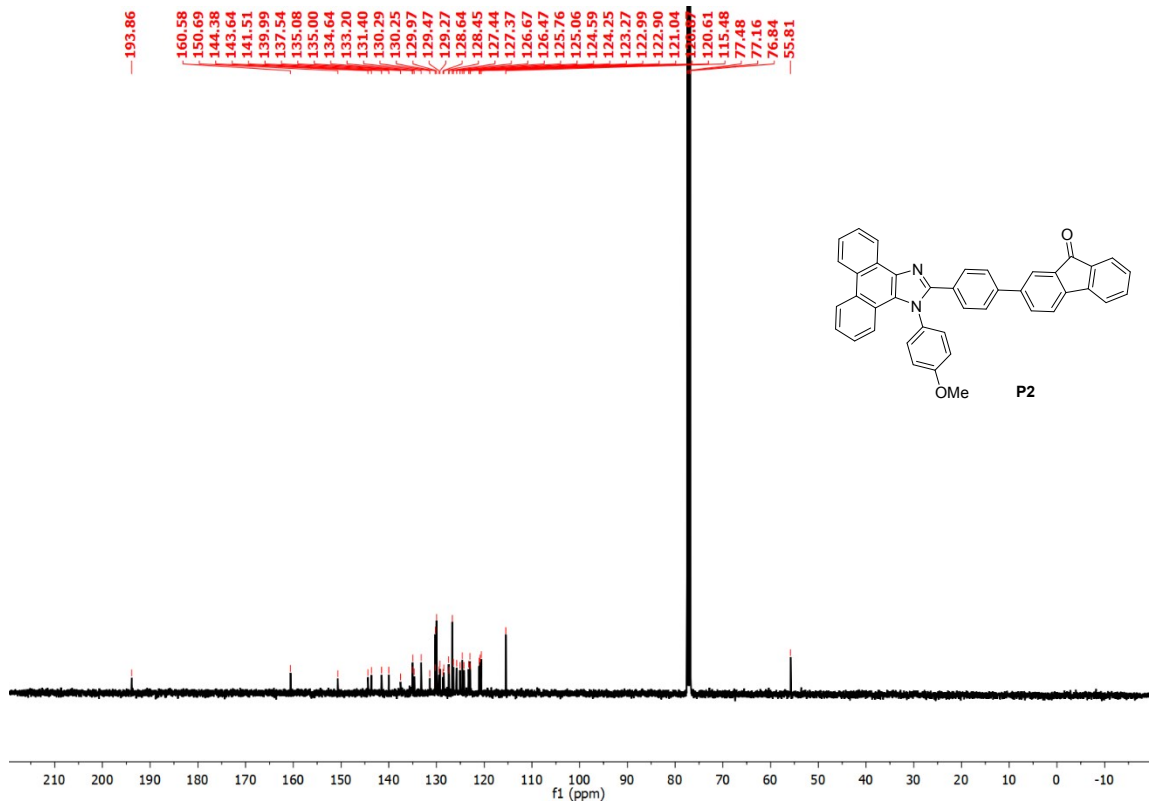

Figure S14:^{13}C NMR Spectrum of compound **P-2** in $CDCl_3$.

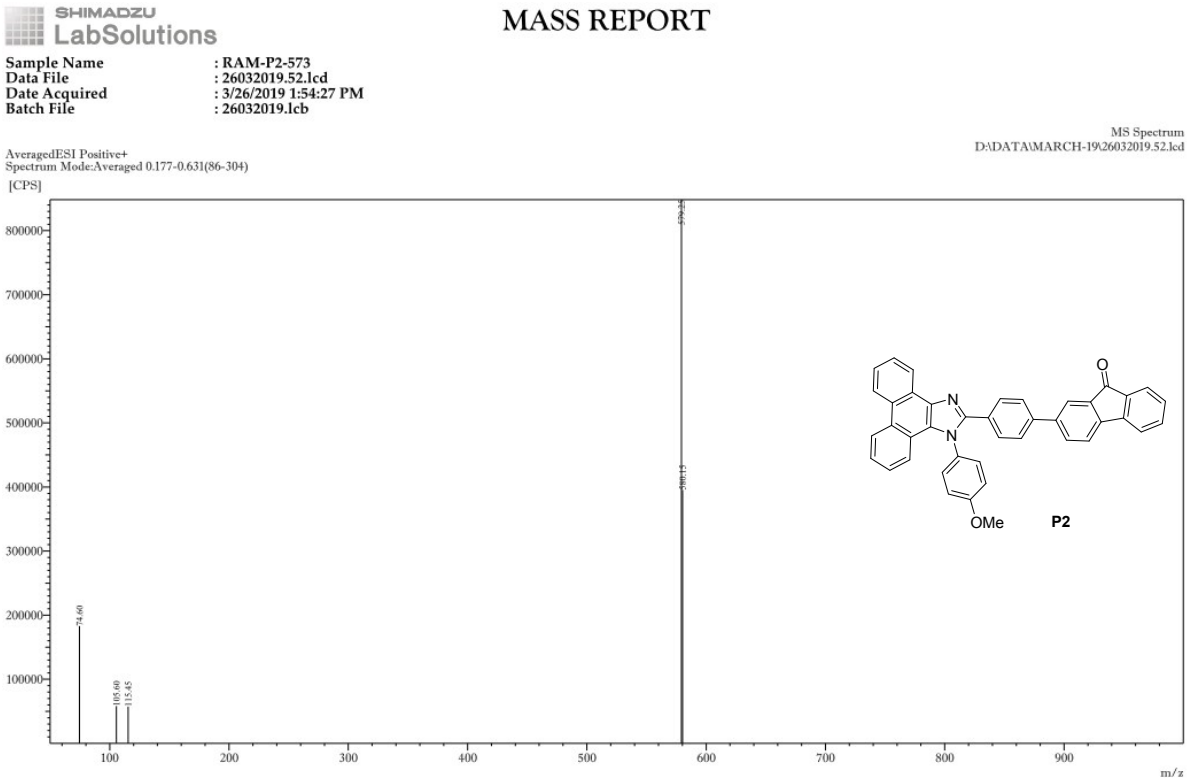

Figure S23: ESI MASS spectra of the luminogen **P-2.**

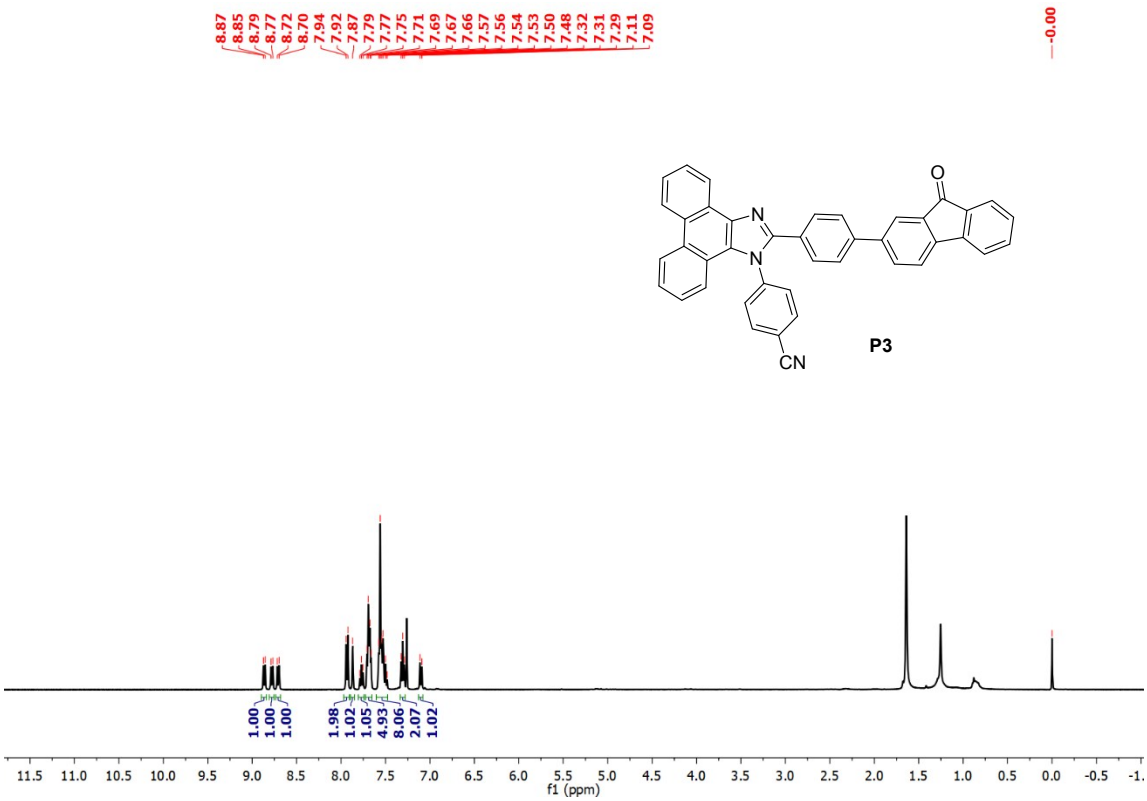

Figure S15: ^{1}H NMR Spectrum of compound **P-3** in $CDCl_3$.

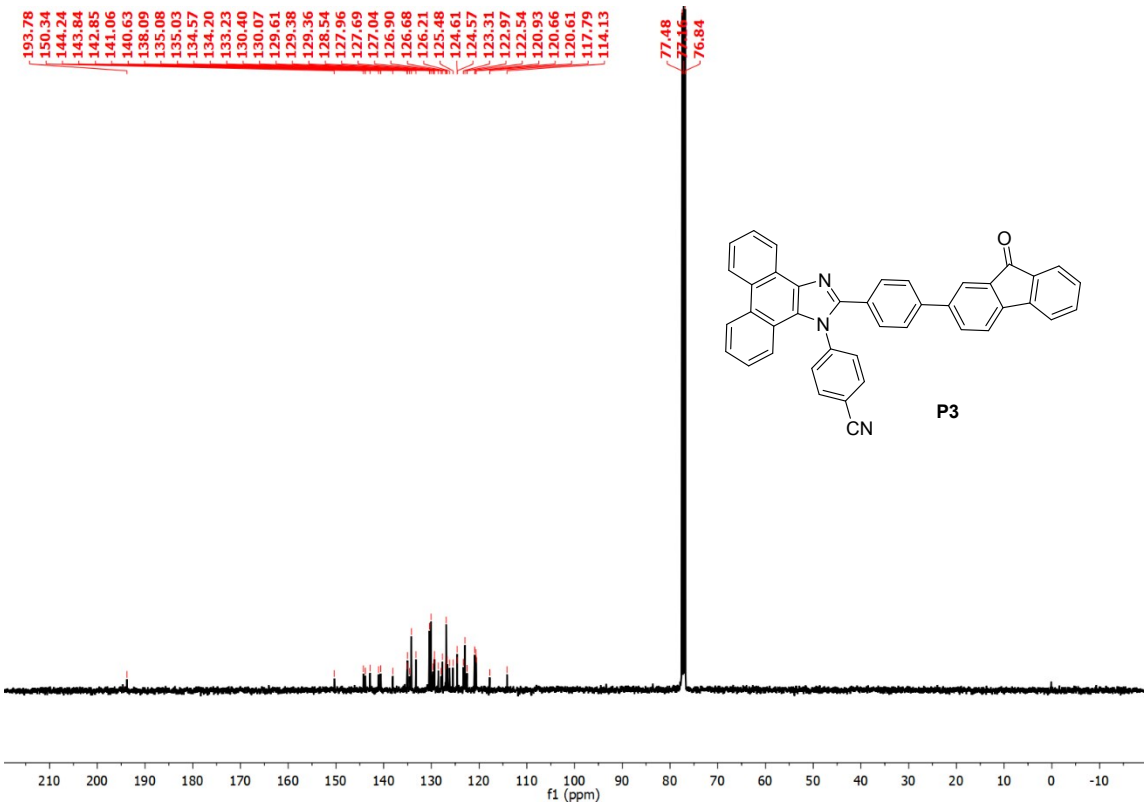

Figure S16: ^{13}C NMR Spectrum of compound **P-3** in $CDCl_3$.

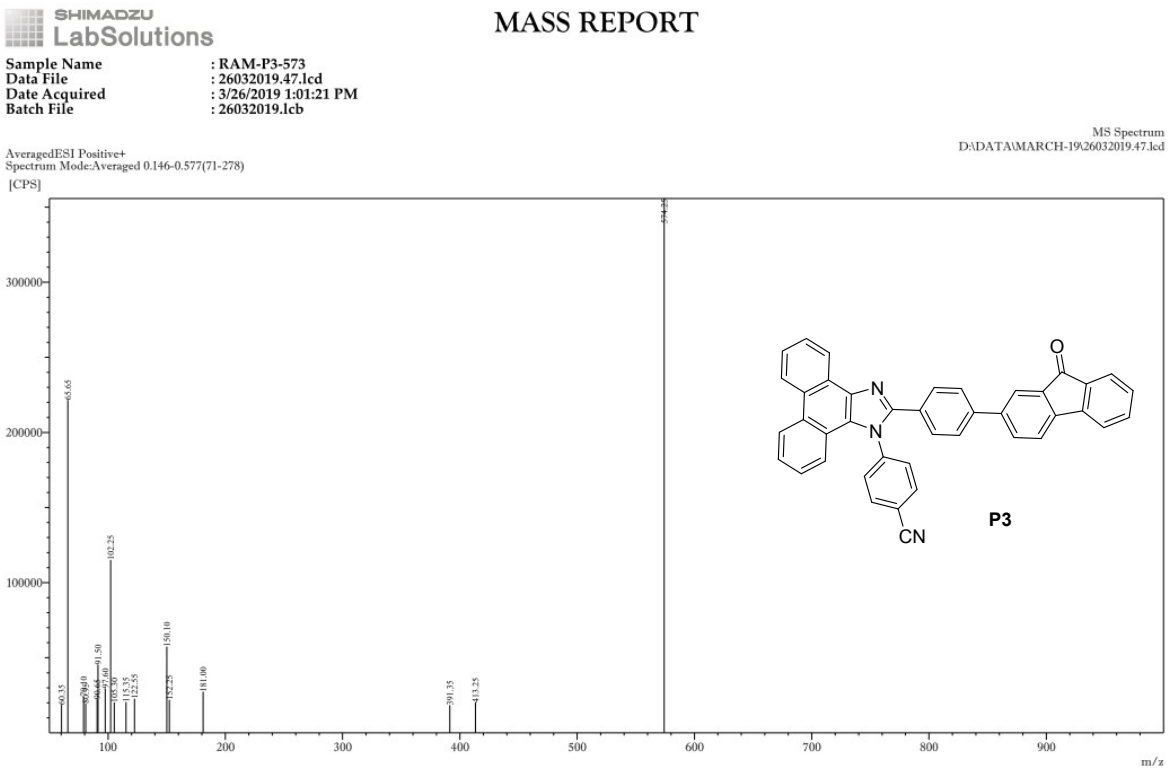

Figure S24: ESI MASS spectra of the luminogen **P-3**.

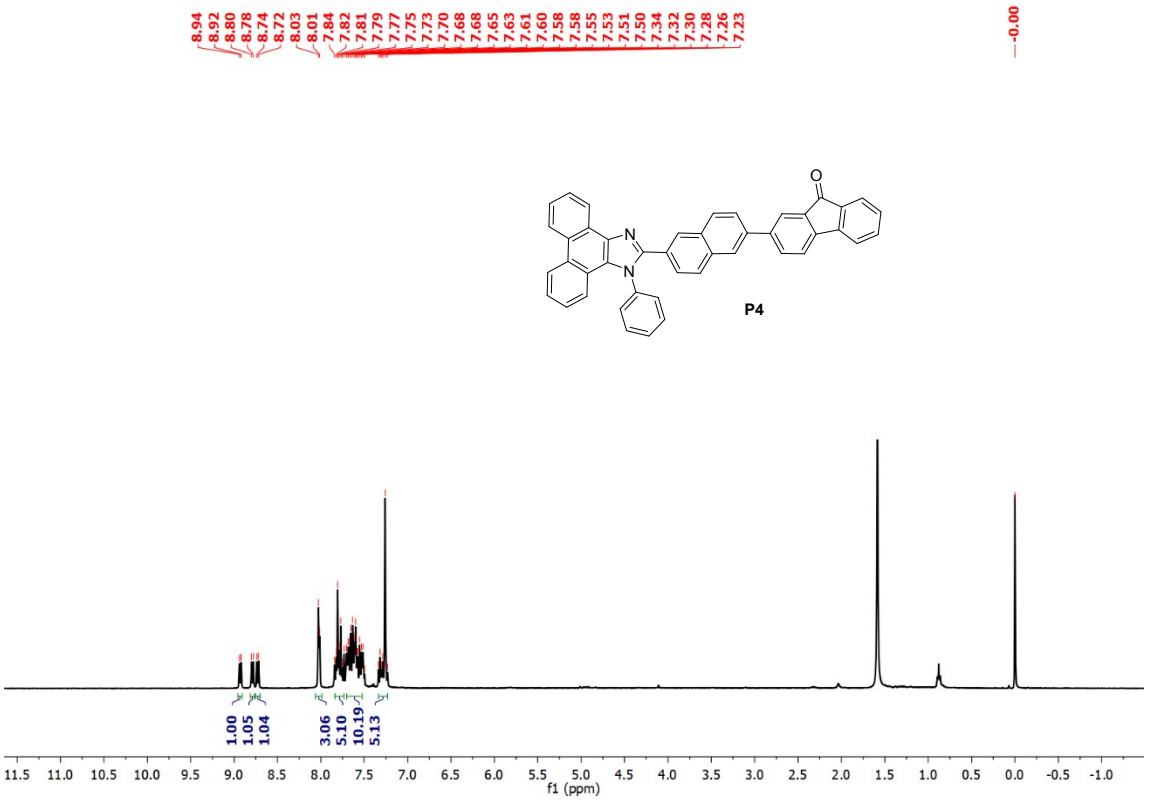

Figure S17: ^{1}H NMR Spectrum of compound **P-4** in $CDCl_3$.

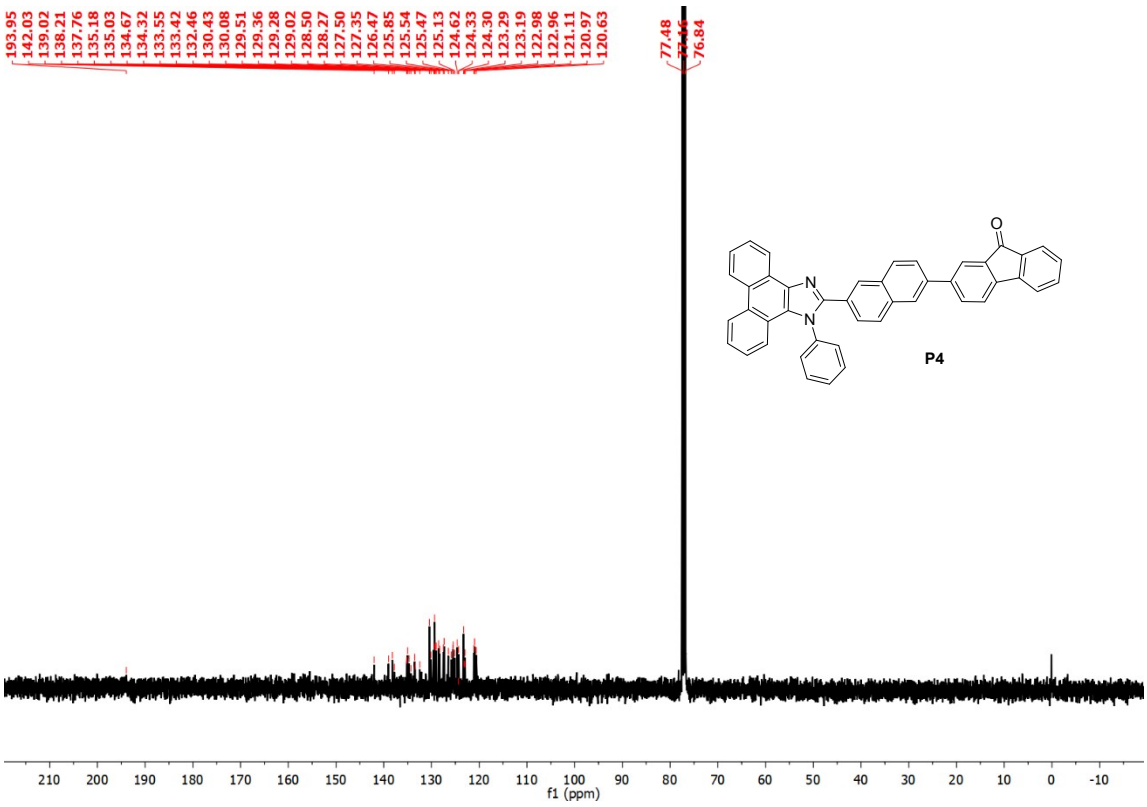

Figure S18: ^{13}C NMR Spectrum of compound **P-4** in $CDCl_3$.

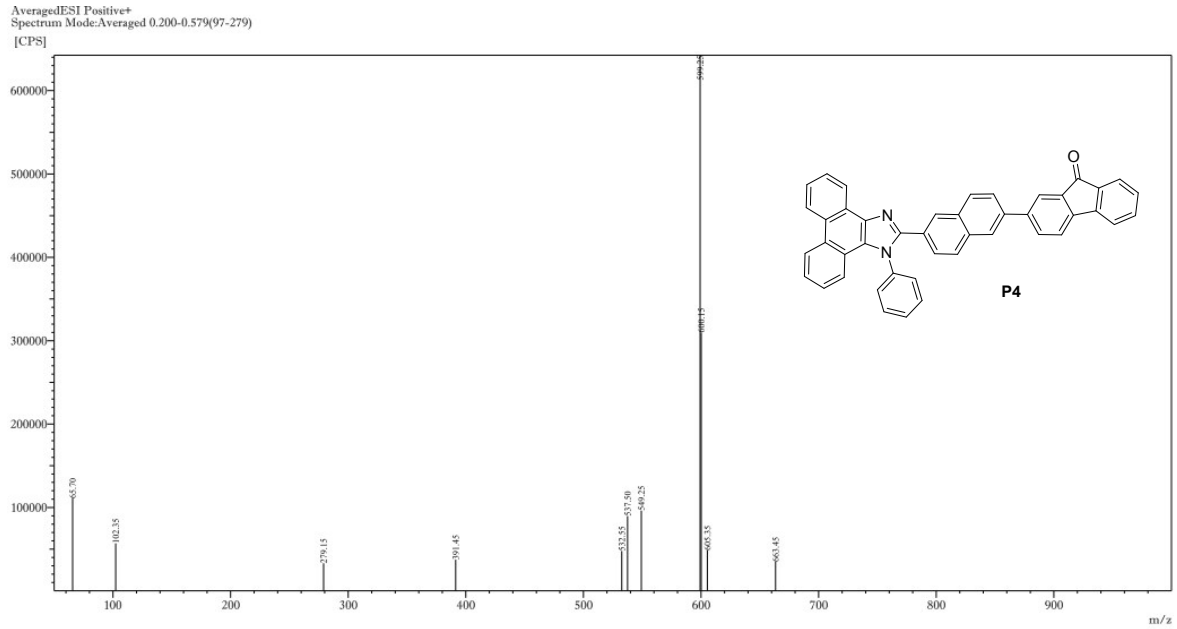

Figure S25: ESI MASS spectra of the luminogen **P-4.**

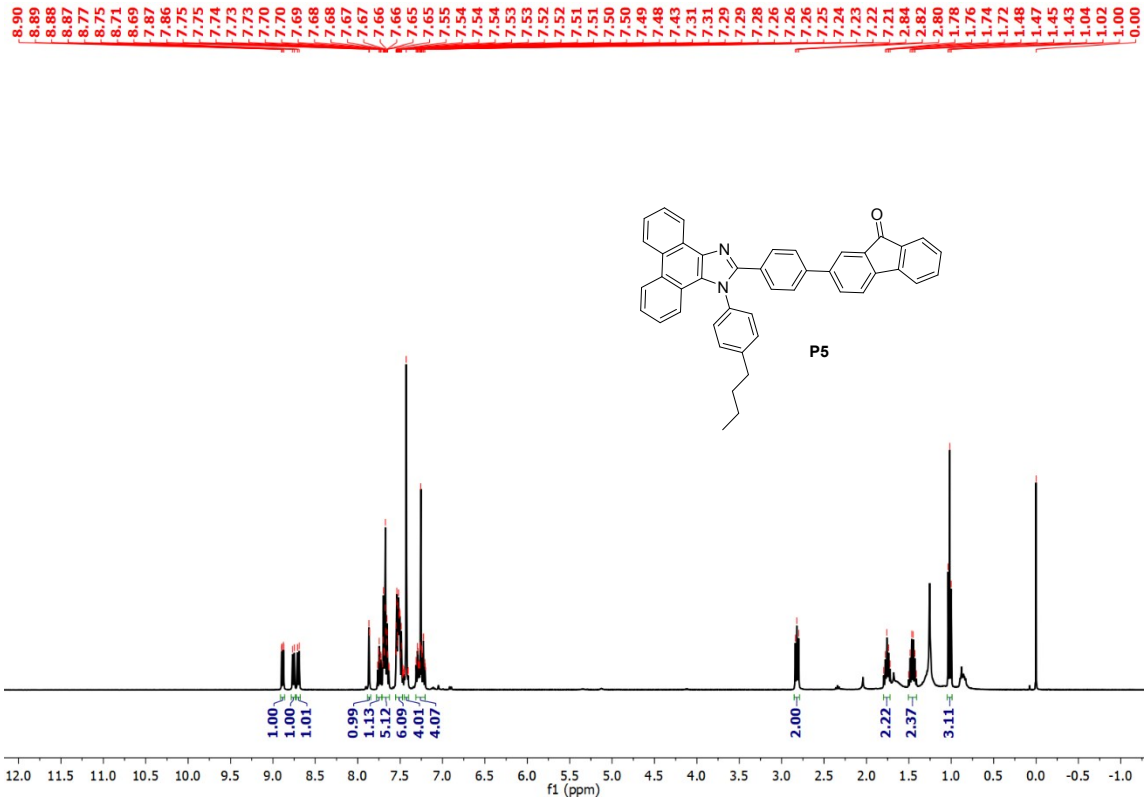

Figure S19: ^{1}H NMR Spectrum of compound **P-5** in $CDCl_3$.

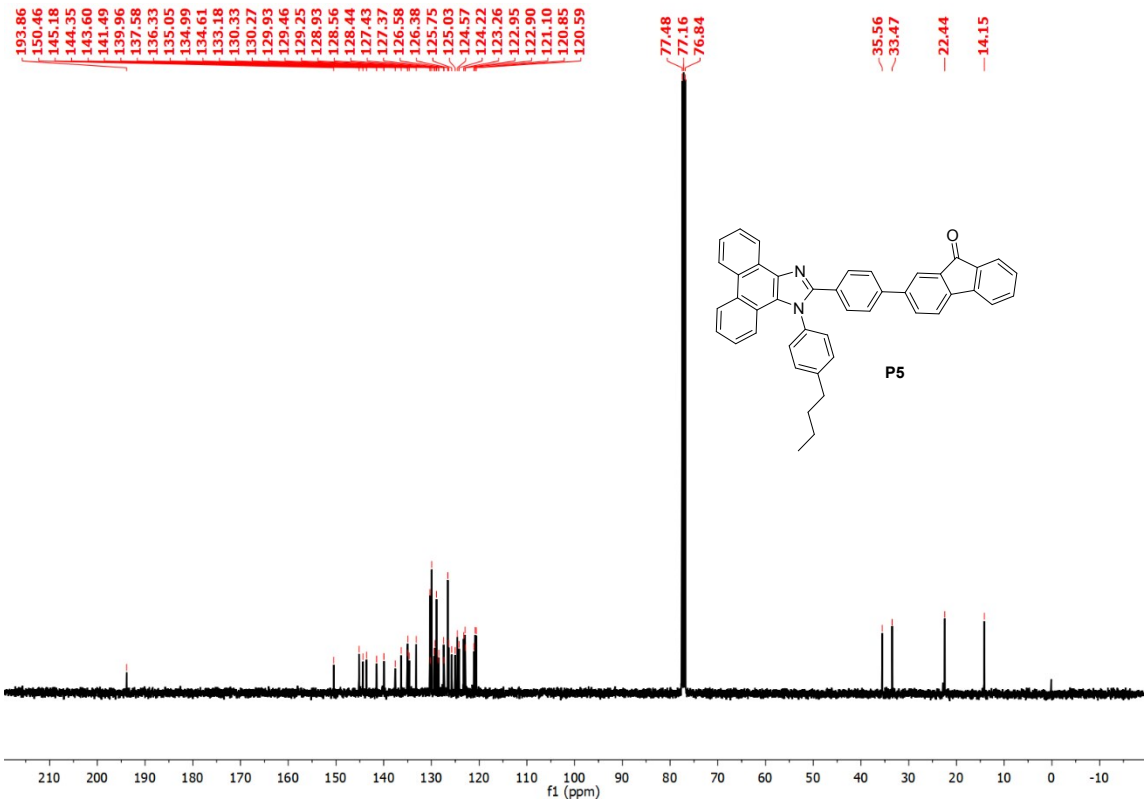

Figure 20 : ^{13}C NMR Spectrum of compound **P-5** in $CDCl_3$.

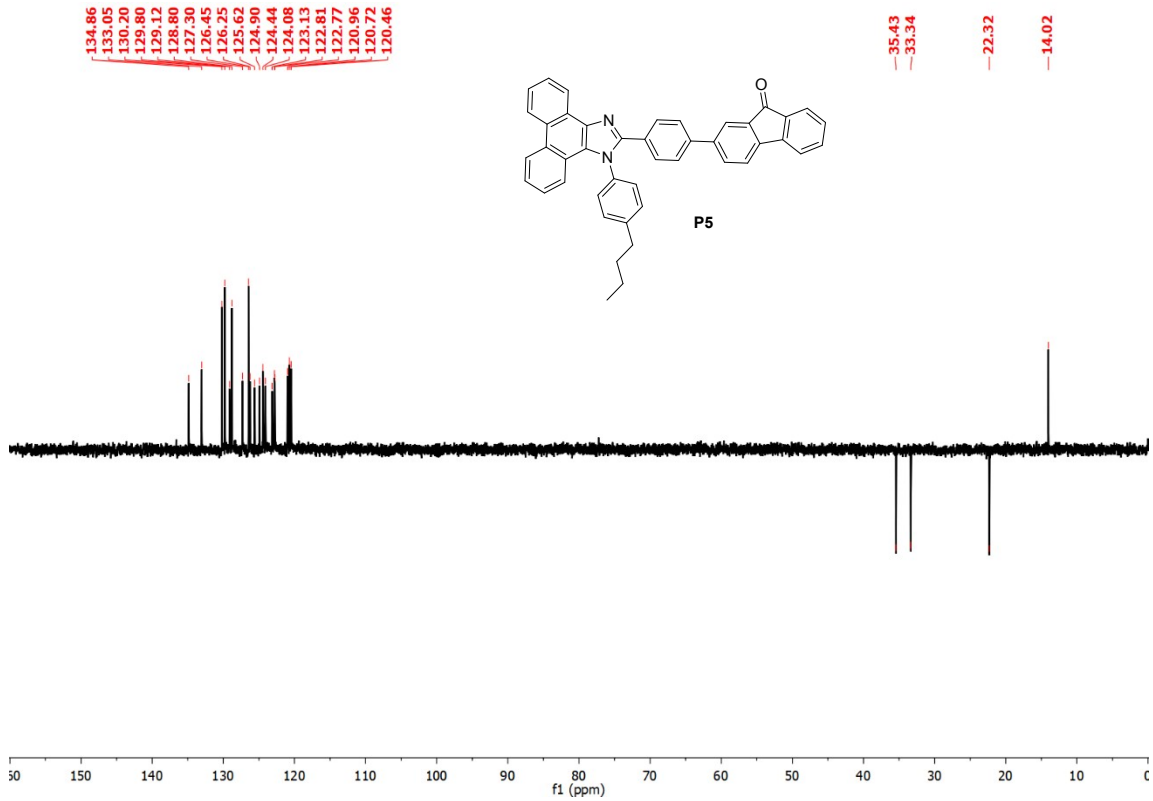

Figure S21: DEPT-135 NMR Spectrum of compound **P-5** in $CDCl_3$.

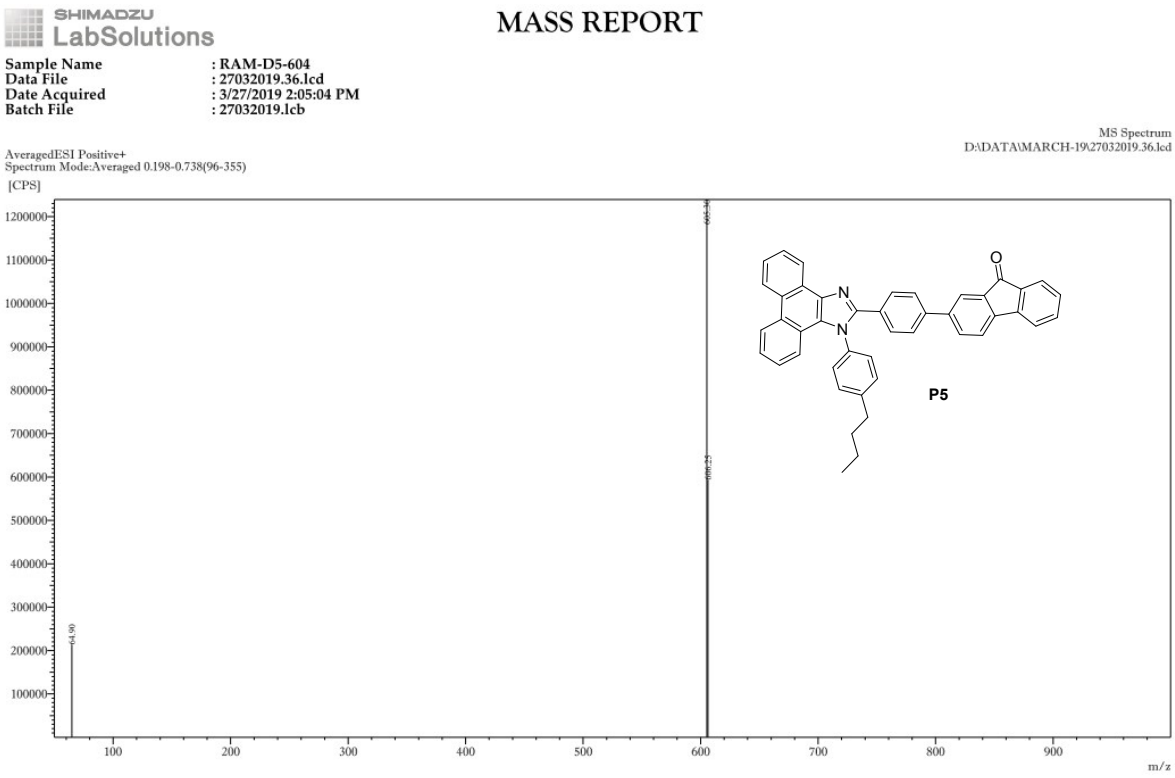

Figure S26: ESI MASS spectra of the luminogen **P-5.**

7. FT-IR Data of the compounds P1-P5

FT-IR measurements were carried out on a Bruker Alpha-P Fourier transform spectrometer and all the measurements were carried out in the solid-state mode.

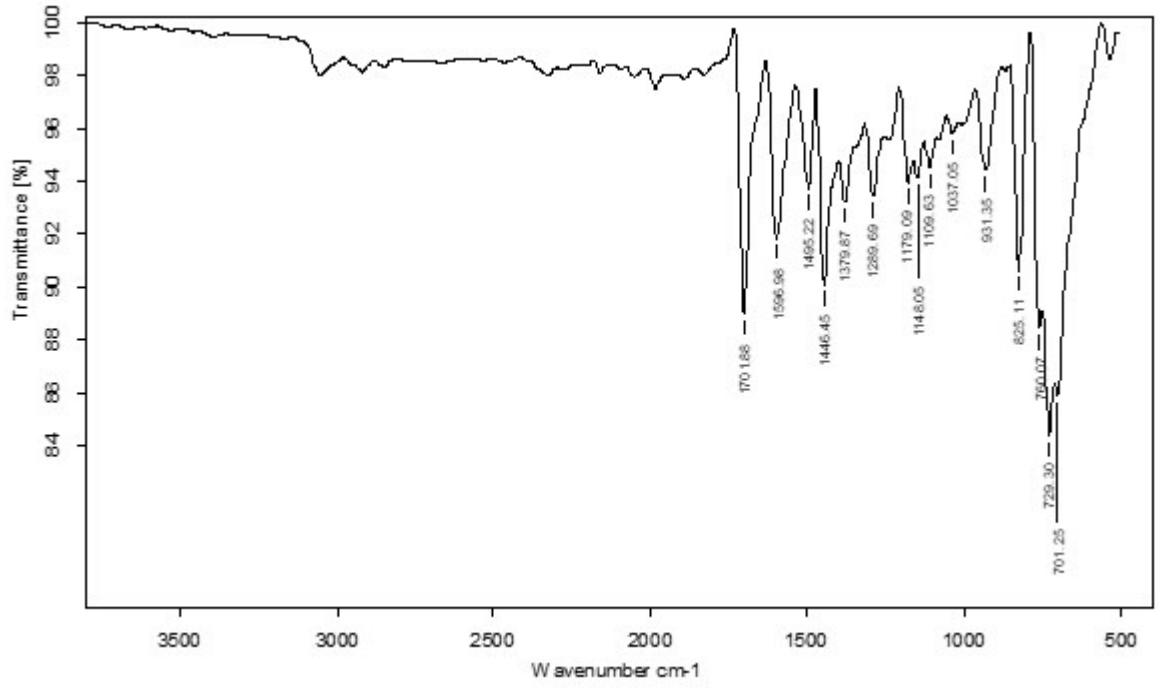

Figure S27: IR Spectrum of the luminogen **P-1.**

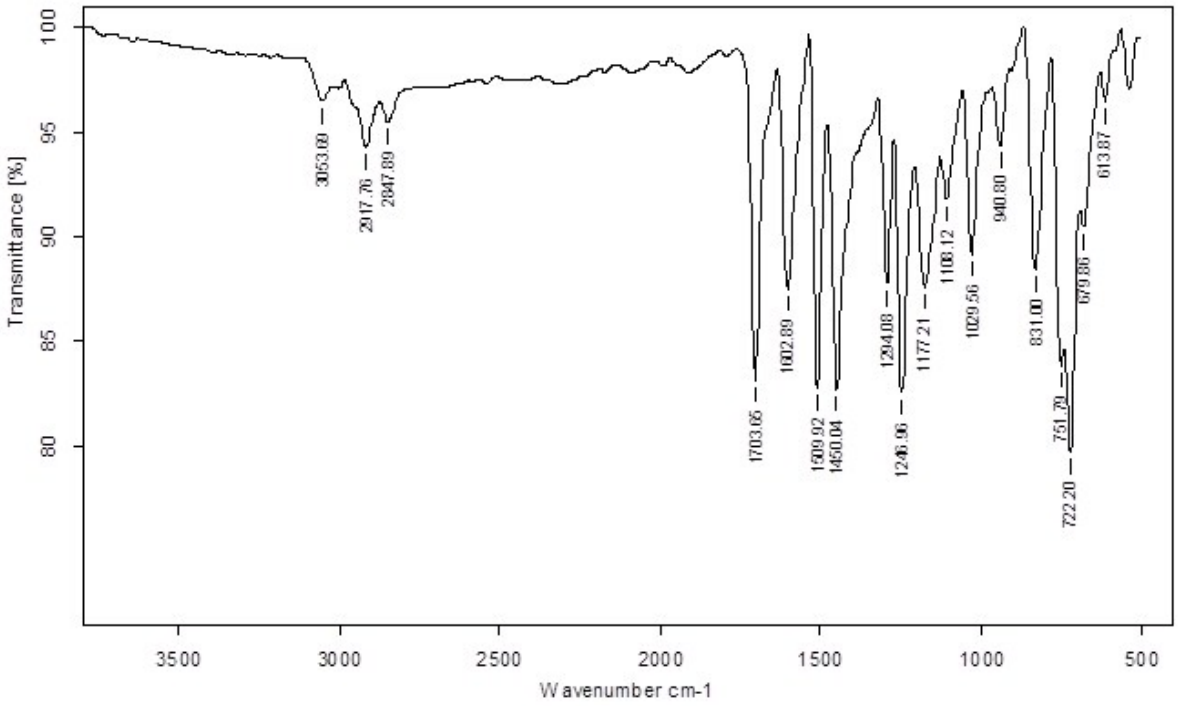

Figure S28: IR Spectrum of the luminogen **P-2.**

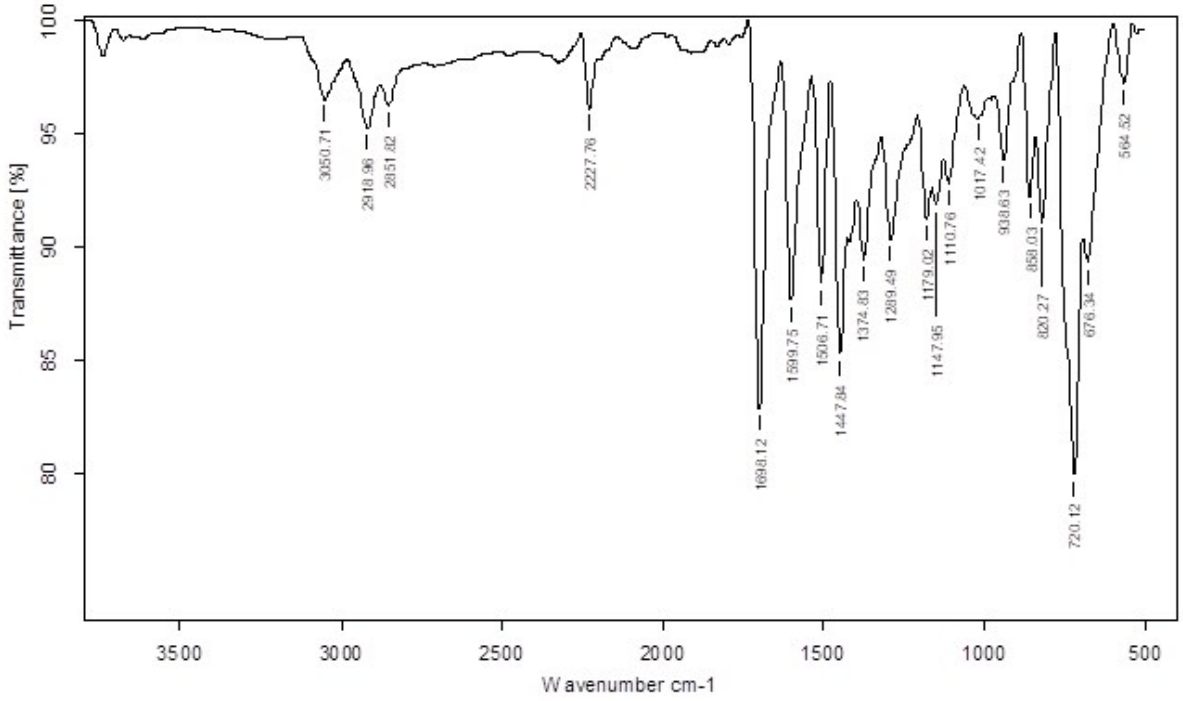

Figure S29: IR Spectrum of the luminogen **P-3.**

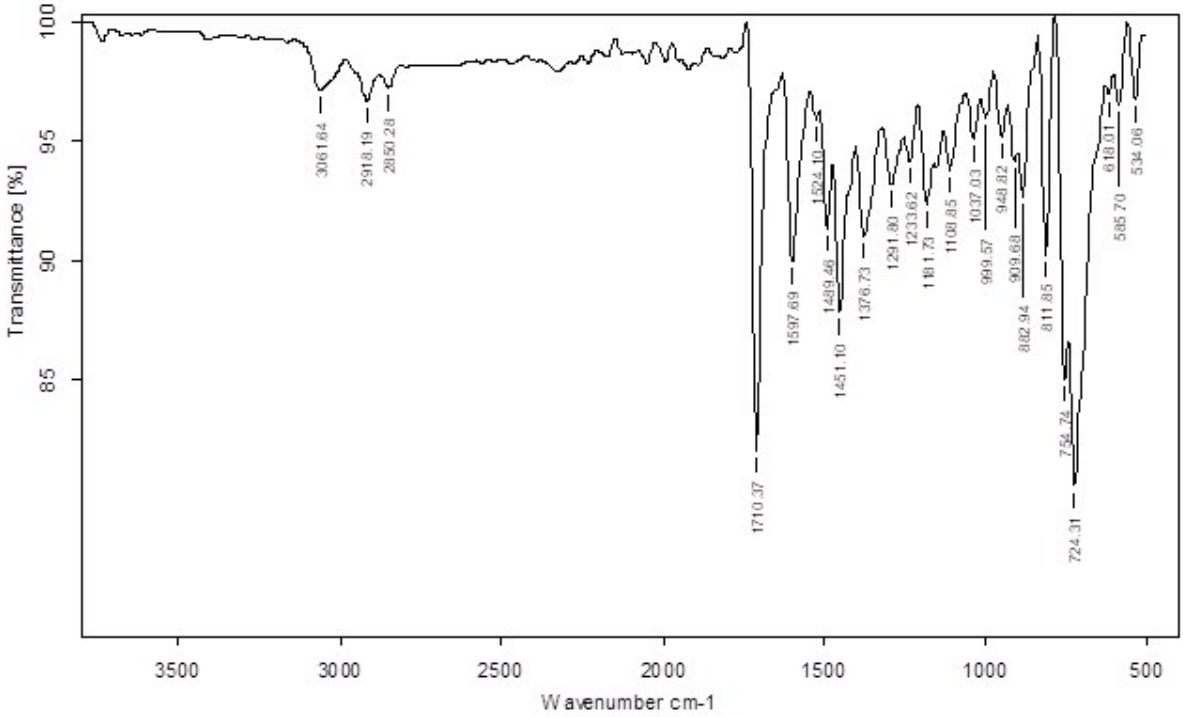

Figure S30: IR Spectrum of the luminogen **P-4.**

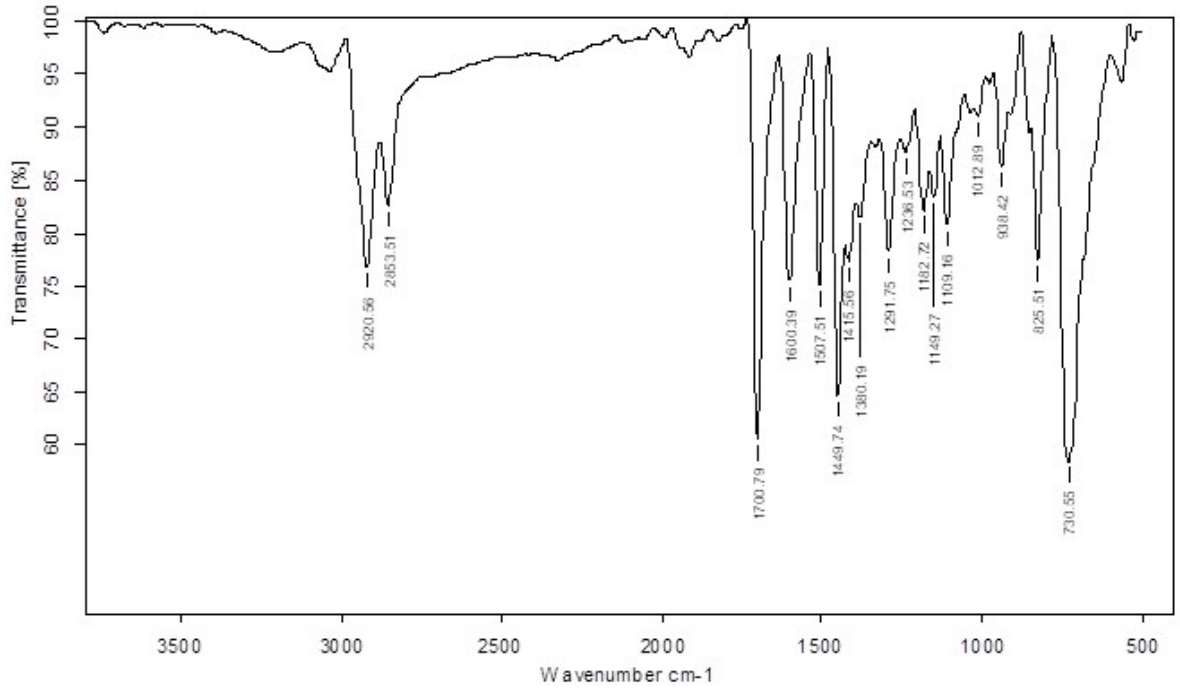

Figure S31: IR Spectrum of the luminogen **P-5.**

8. Molecular Structure and Crystal Packing

Single crystals of $C_{82}H_{46}N_6O_2$ **P2** was recorded. A suitable crystal was selected and mounted on a **SuperNova, Dual, Cu at home/near, Eos** diffractometer. The crystal was kept at 293 K during data collection. Using Olex2 [1], the structure was resolved with the ShelXS [2] structure solution program using Direct Methods and refined with the olex2.refine [3] refinement package using Gauss-Newton minimization. (Mo Kα (λ = 0.71073)).

1. Dolomanov, O.V., Bourhis, L.J., Gildea, R.J, Howard, J.A.K. & Puschmann, H. (2009), J. *Appl. Cryst.* 42, 339-341.
2. Sheldrick, G.M. (2008). *Acta Cryst*. A64, 112-122.
3. Bourhis, L.J., Dolomanov, O.V., Gildea, R.J., Howard, J.A.K., Puschmann, H. (2015). *Acta Cryst. A*71, 59-75.

Table 1: Crystal data and structure refinement for P-3	
Identification code	P3 (9891)
CCDC No.	1947005
Empirical formula	$C_{82}H_{46}N_6O_2$
Formula weight	1252.43
Temperature/K	293
Crystal system	triclinic
Space group	P-1
a/Å	8.5508(7)
b/Å	20.5520(17)
c/Å	20.7183(18)
α/°	67.182(8)
β/°	82.780(7)
γ/°	78.538(7)
Volume/Å^3	3284.3(5)
Z	2
ρ_{calc}g/cm^3	1.2663
μ/mm^{-1}	0.079
F(000)	1306.6
Crystal size/mm^3	0.07 × 0.05 × 0.03
Radiation	Mo Kα (λ = 0.71073)
2Θ range for data collection/°	4.08 to 58.2
Index ranges	-10 ≤ h ≤ 11, -27 ≤ k ≤ 27, -23 ≤ l ≤ 27
Reflections collected	27160
Independent reflections	14933 [R_{int} = 0.0617, R_{sigma} = 0.1631]
Data/restraints/parameters	14933/0/874
Goodness-of-fit on F^2	1.054
Final R indexes [I>=2σ (I)]	R_1 = 0.0988, wR_2 = 0.2211
Final R indexes [all data]	R_1 = 0.2669, wR_2 = 0.3292
Largest diff. peak/hole / e Å^{-3}	0.75/-0.66

9. DFT Calculations

Density functional theory (DFT) calculation of the compounds from P1-P5 were carried out using Gaussian 09 program package. The ground state geometries of these luminogens were optimized using DFT-B3LYP-6-311G basis set. To obtain the information on absorption properties, Time-dependent density functional theory (TDDFT) calculations were performed using the optimized geometries.

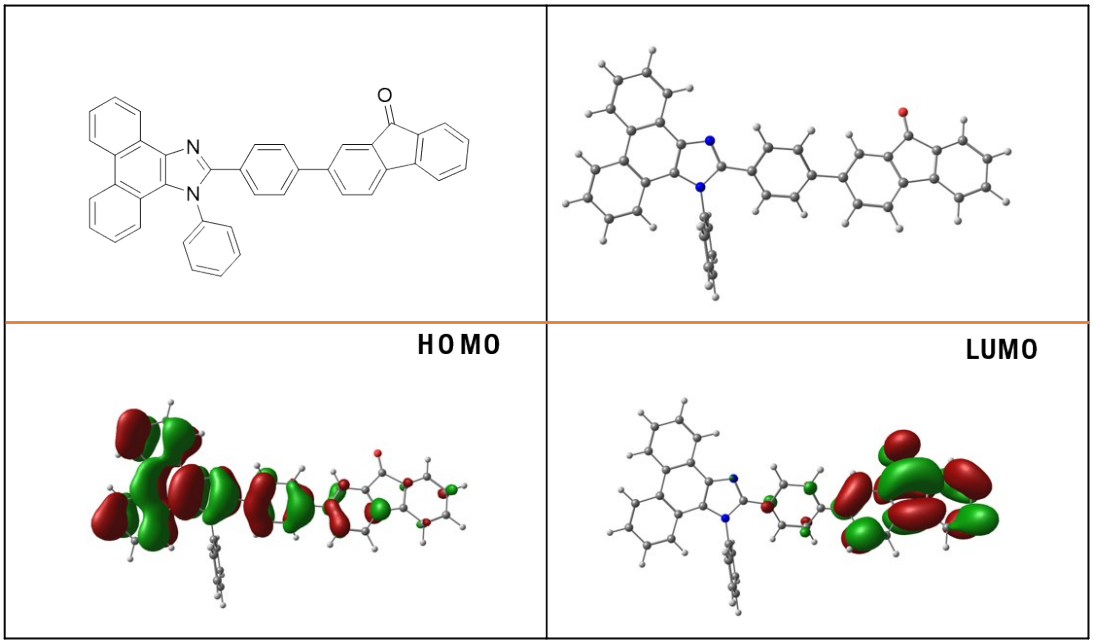

Figure S32: HOMO-LUMO of the luminogen P1.

Energy gap: 2.8663485938698 Ev

HOMO Energy: -5.2693384711136 eV

LUMO energy: -2.4029898772438 eV

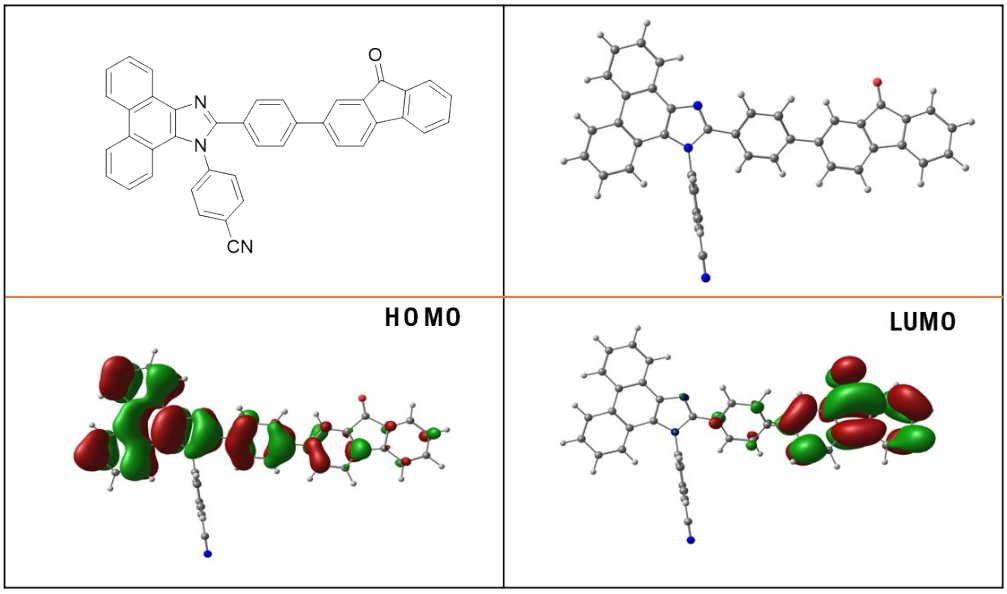

Figure S33: HOMO-LUMO of the luminogen P2.

Energy gap: 3.00957178094872 eV

HOMO Energy: -5.4946927515168 eV

LUMO energy: -2.48512097056808 Ev

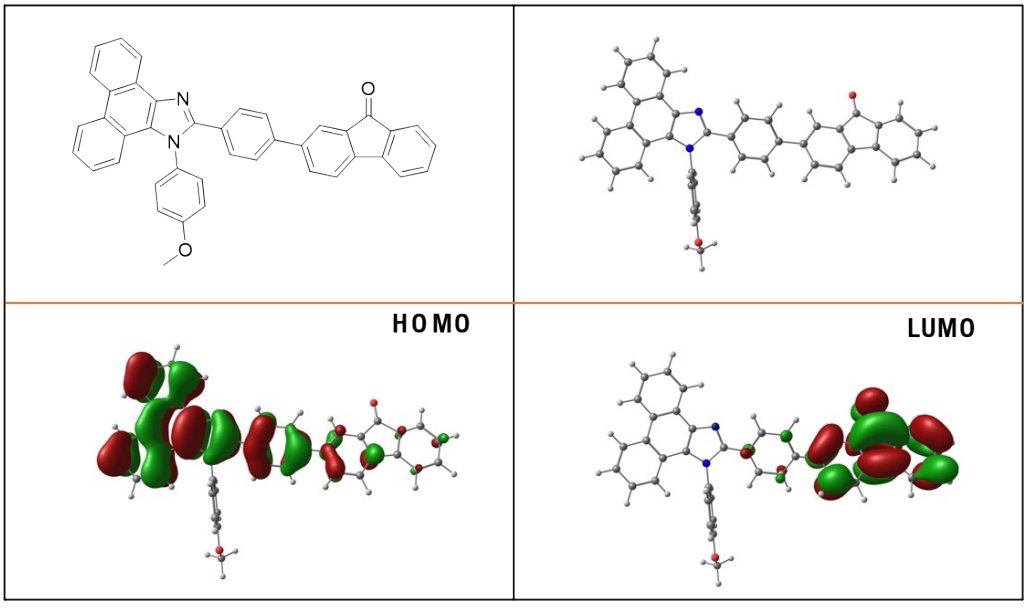

Figure S34: HOMO-LUMO of the luminogen P3.

Energy gap: 2.8436337515872 eV

HOMO Energy: -5.229600936248 eV

LUMO energy: -2.3859671846608 eV

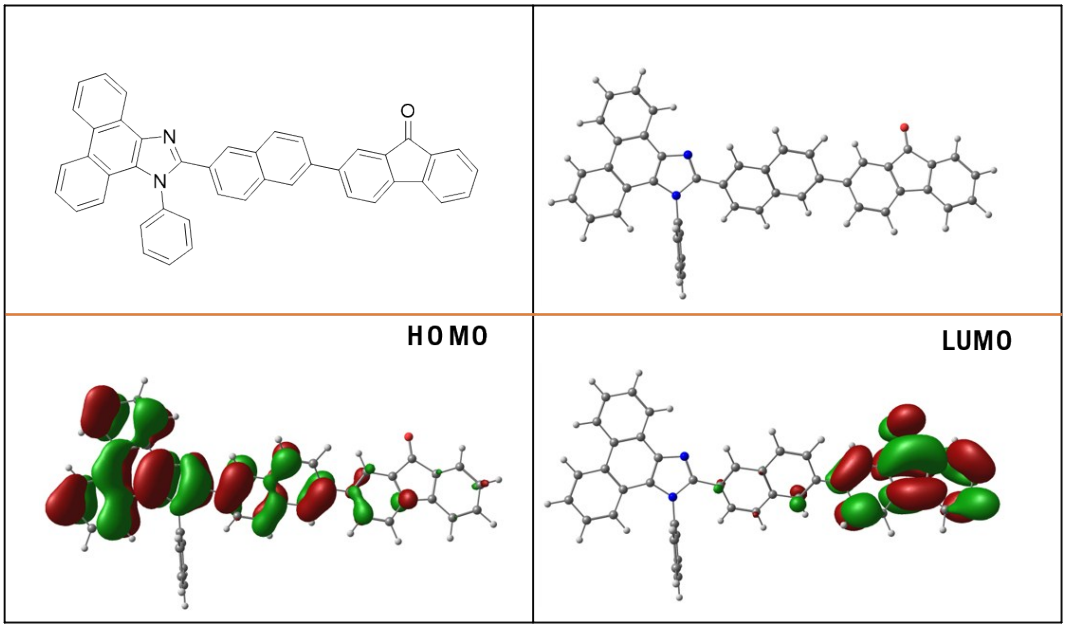

Figure S35: HOMO-LUMO of the luminogen P4.

Energy gap: 2.813702910005 eV

HOMO Energy: -5.2278919389216 eV

LUMO energy: -2.4141890289166 eV

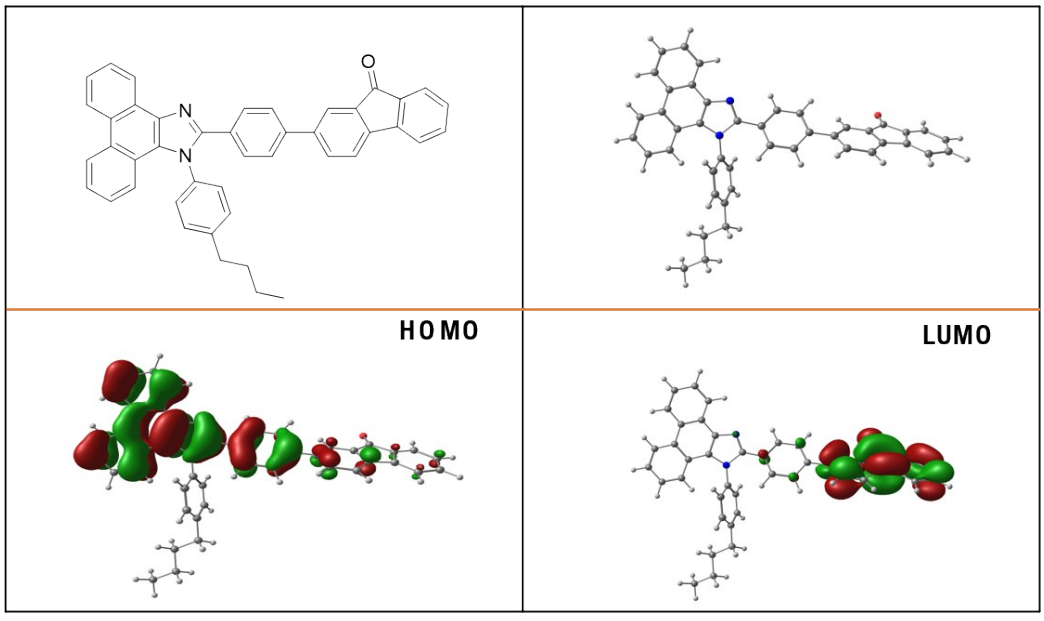

Figure S36: HOMO-LUMO of the luminogen P5.

Energy gap: 2.8377205620608 eV

HOMO Energy: -5.231391187412 eV

LUMO energy: -2.3936706253512 eV

10. Cyclic voltammetry compound P1-P5

Cyclic voltammograms (CV) of all the luminogen P1-P5, and the position of the CB and VB energy levels were calculated from the oxidation and reduction potential. These measurements were recorded in an aqueous 0.1 M DCM solution. Among these three cells, a glassy carbon electrode and platinum electrode were utilized as a working and counter electrode respectively. For the reference electrode, Ag/AgCl electrode was utilized.

The lowest unoccupied molecular orbital (LUMO) and the highest occupied molecular orbital (HOMO) positions were calculated by using the following method.

For P1:

E_{red} = –2.49 V versus Ag/AgCl/KCl

Electrode potential of reference electrode = +0.197 V

E_{red} versus NHE (normal hydrogen electrode)

E_{red} = –2.49 V + 0.197 V = –2.29 V (NHE)

We converted V (volts) into eV (electron volts),

Therefore E_{red} = –4.5 eV (0 V vs NHE) – (–2.29 V) = –2.21 eV (LUMO)

Then the HOMO position was obtained by the addition of the optical bandgap energy value to the LUMO energy.

E_{red} = –2.21 eV – 2.86 eV = –5.07 eV (HOMO)

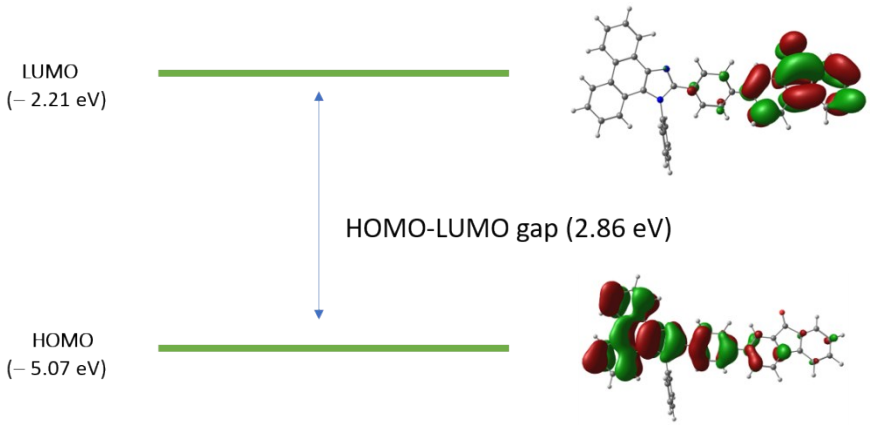

For P2:

E_{red} = –2.33 V versus Ag/AgCl/KCl

Electrode potential of reference electrode = +0.197 V

E_{red} versus NHE (normal hydrogen electrode)

E_{red} = –2.33 V + 0.197 V = –2.133 V (NHE)

We converted V (volts) into eV (electron volts),

Therefore E_{red} = –4.5 eV (0 V vs NHE) – (–2.133 V) = –2.36 eV (LUMO)

Then the HOMO position was obtained by the addition of the optical bandgap energy value (DFT) to the LUMO energy.

E_{red} = –2.36 eV – 2.48 eV = –4.84 eV (HOMO)

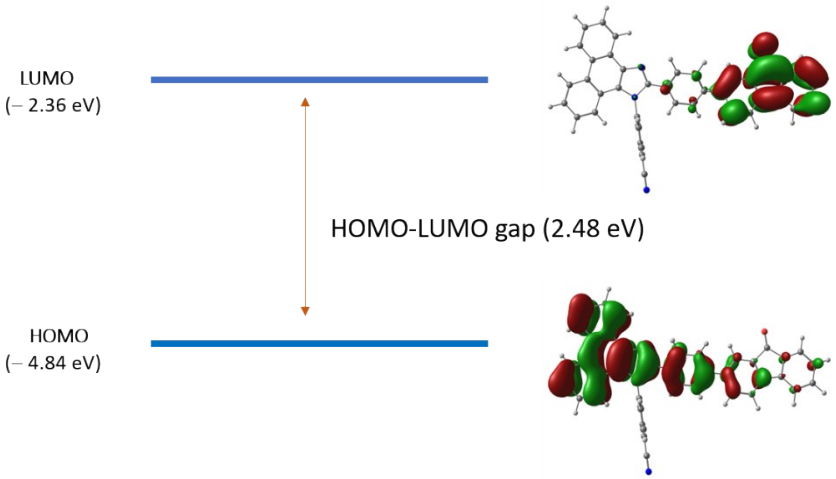

For P3:

E_{red} = –2.1 V versus Ag/AgCl/KCl

Electrode potential of reference electrode = +0.197 V

E_{red} versus NHE (normal hydrogen electrode)

E_{red} = –2.49 V + 0.197 V = –1.903 V (NHE)

We converted V (volts) into eV (electron volts),

Therefore E_{red} = –4.5 eV (0 V vs NHE) – (–1.903 V) = –2.59 eV (LUMO)

Then the HOMO position was obtained by the addition of the optical bandgap energy value to the LUMO energy.

E_{red} = –2.59 eV – 2.84 eV = –5.44 eV (HOMO)

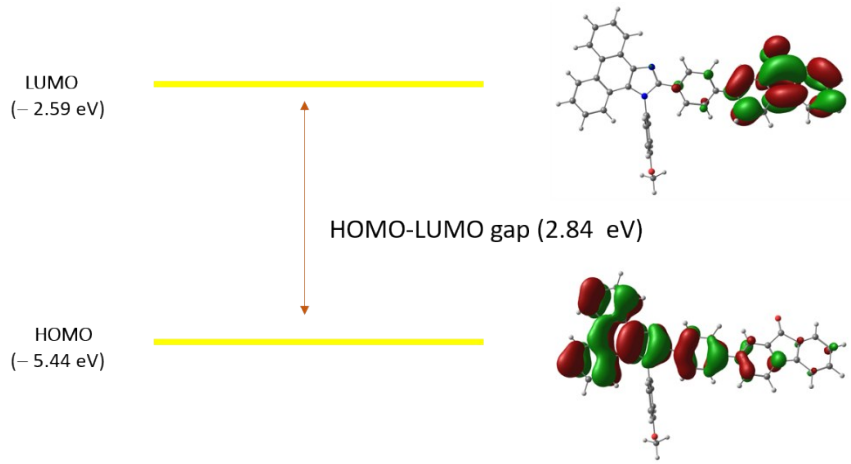

For P4:

E_{red} = –2.39 V versus Ag/AgCl/KCl

Electrode potential of reference electrode = +0.197 V

E_{red} versus NHE (normal hydrogen electrode)

E_{red} = –2.39 V + 0.197 V = –2.19 V (NHE)

We converted V (volts) into eV (electron volts),

Therefore E_{red} = –4.5 eV (0 V vs NHE) – (–2.19 V) = –2.30 eV (LUMO)

Then the HOMO position was obtained by the addition of the optical bandgap energy value to the LUMO energy.

E_{red} = –2.81 eV – 2.30 eV = –5.12 eV (HOMO)

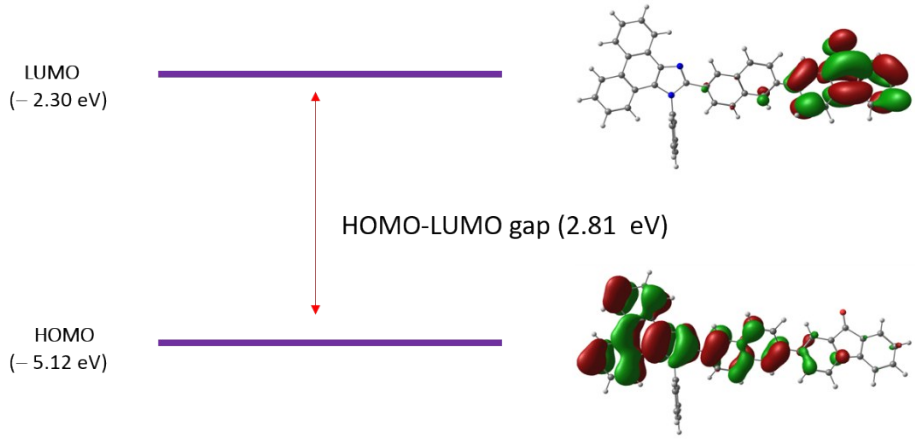

For P5:

E_{red} = –2.37 V versus Ag/AgCl/KCl

Electrode potential of reference electrode = +0.197 V

E_{red} versus NHE (normal hydrogen electrode)

$$E_{red} = -2.37\ V + 0.197\ V = -2.17\ V\ (NHE)$$

We converted V (volts) into eV (electron volts),

$$\text{Therefore } E_{red} = -4.5\ eV\ (0\ V\ vs\ NHE) - (-2.17\ V) = -2.32\ eV\ (LUMO)$$

Then the HOMO position was obtained by the addition of the optical bandgap energy value to the LUMO energy.

$$E_{red} = -2.32\ eV - 2.83\ eV = -5.16\ eV\ (HOMO)$$

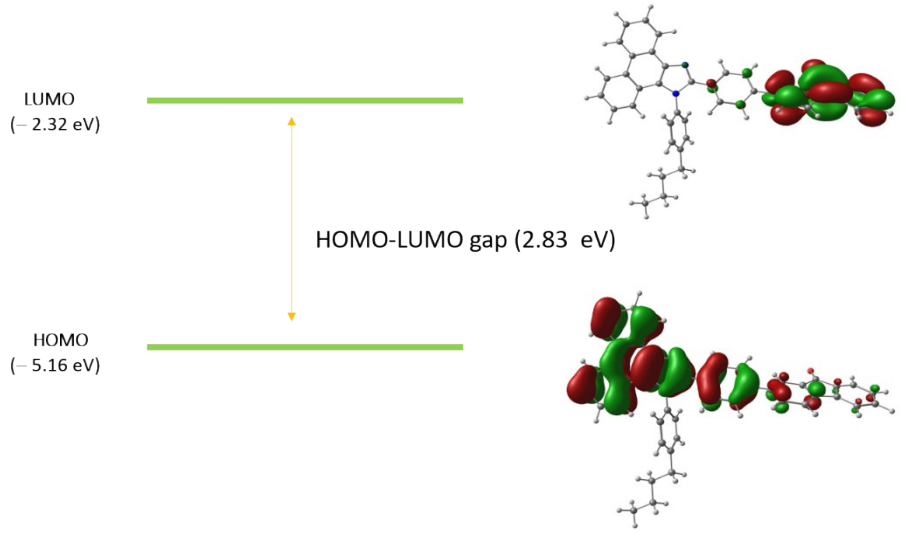

11. Photoluminescence Studies

11.1 Absorption and Fluorescent spectra of synthesised compounds

The steady state and time resolved photoluminescence properties of 2 using fluorescence spectrometer from Edinburgh Instruments (FLS 1000) was investigated. For steady state luminescence measurement, the sample was exited using 380 and 420 nm collimated beam from the excitation monochromator of the spectrometer, which is pumped using a 450 W Xe2 continuous xenon lamp. The emission spectrum after passing through emission monochromator is scanned and detected in high-gain red sensitive photomultiplier (PMT) detector with spectral coverage from 400 nm to ~ 800 nm. The luminescence lifetime was measured using standard time-correlated single photon counting (TCSPC) technique using picosecond pulsed diode laser of wavelength 405 nm from Edinburgh Instruments (EPL-405) with repetition rate 200 KHz. The decay is fitted using reconvolution fit analysis using the IRF to extract the life-time parameters from the whole time resolved measurement.

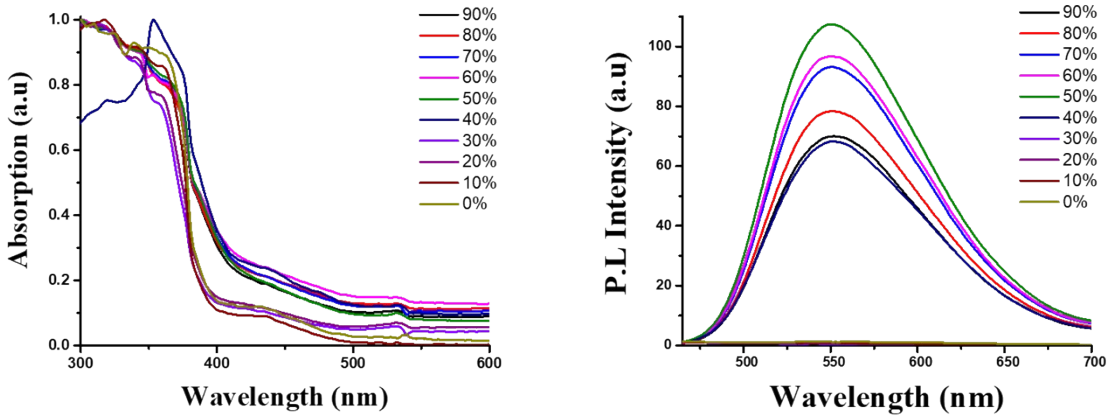

Figure S37: (a) Absorption (b) PL spectrum of **P2** in DMSO/Water mixtures with varying water fraction(*fw*); Con-10µM; Excitation wavelength-380 nm.

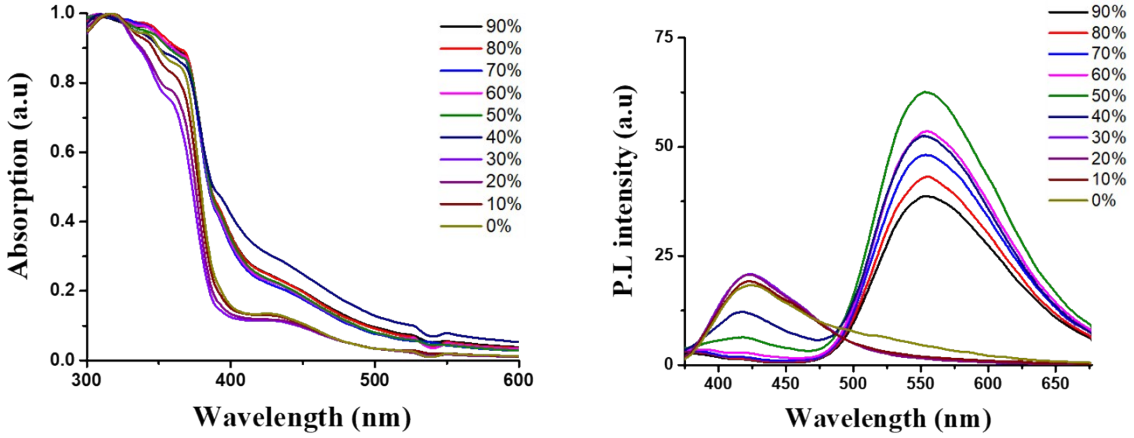

Figure S38: (a) Absorption (b) PL spectrum of **P3** in DMSO/Water mixtures with varying water fraction(*fw*); Con-10µM; Excitation wavelength-380 nm.

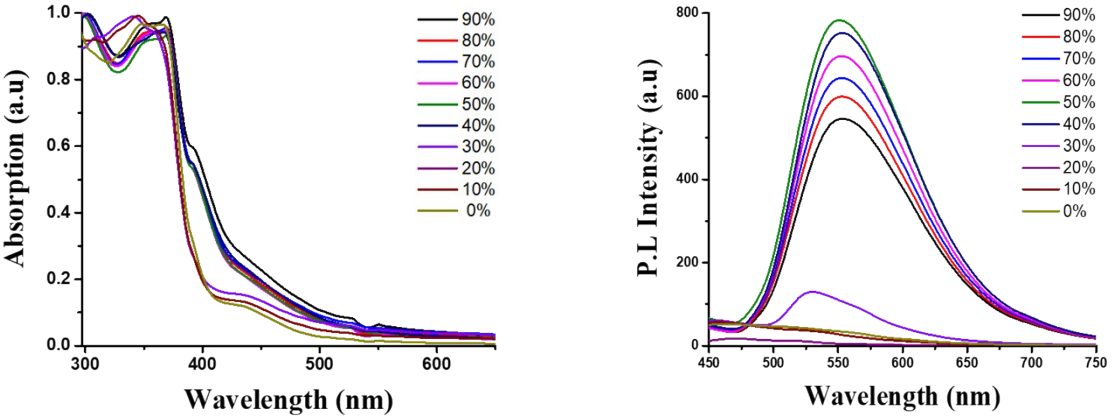

Figure S39: (a) Absorption (b) PL spectrum of **P4** in DMSO/Water mixtures with varying water fraction(*fw*); Con-10µM; Excitation wavelength-380 nm.

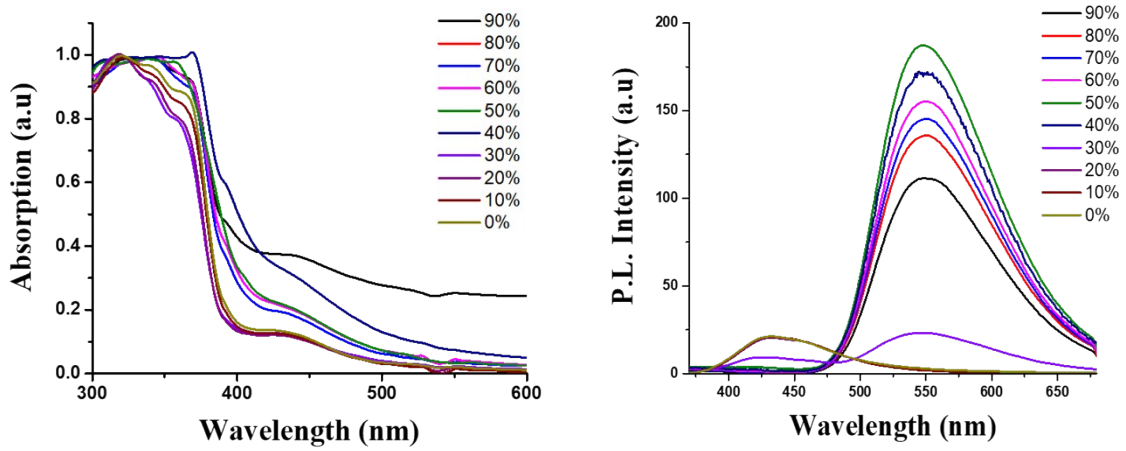

Figure S40: (a) Absorption (b) PL spectrum of **P5** in DMSO/Water mixtures with varying water fraction(*fw*); Con-10μM; Excitation wavelength-380 nm.

11.2 3D fluorescence spectrum

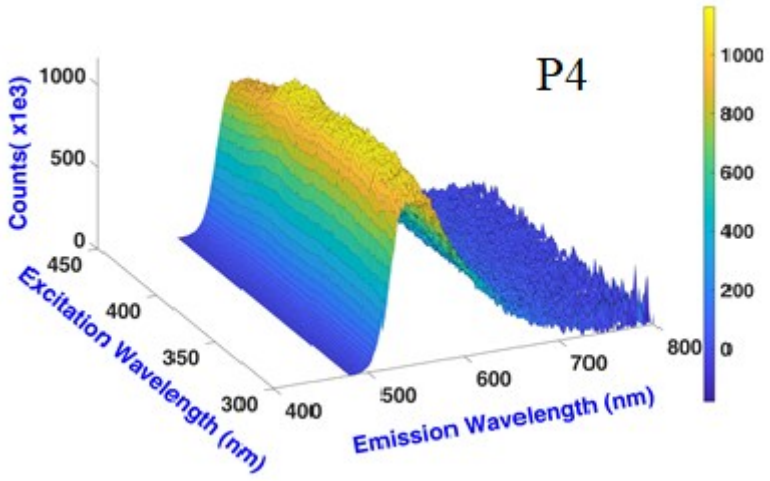

Figure S41: The 3D fluorescence spectrum of P4 in thin film state.

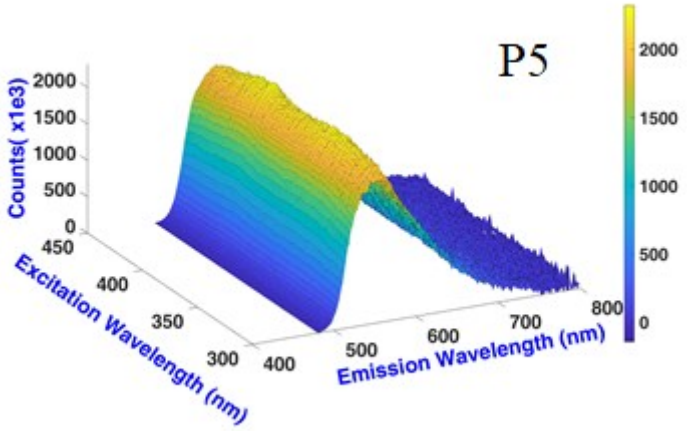

Figure S42: The 3D fluorescence spectrum of P5 in thin film state.

11.3 Emission spectra (PL) at 405 nm

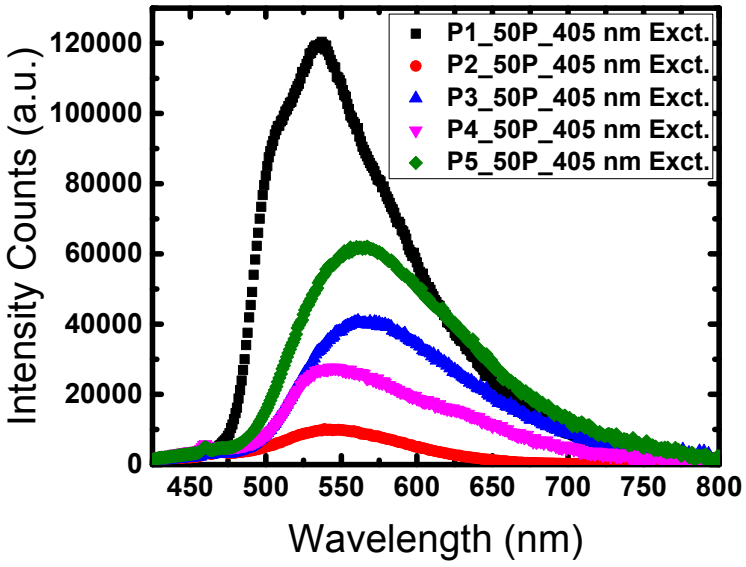

Figure S43: Emission Scan (PL) at 405 nm Excitation for P1-P5 Samples (*fw*-50 %).

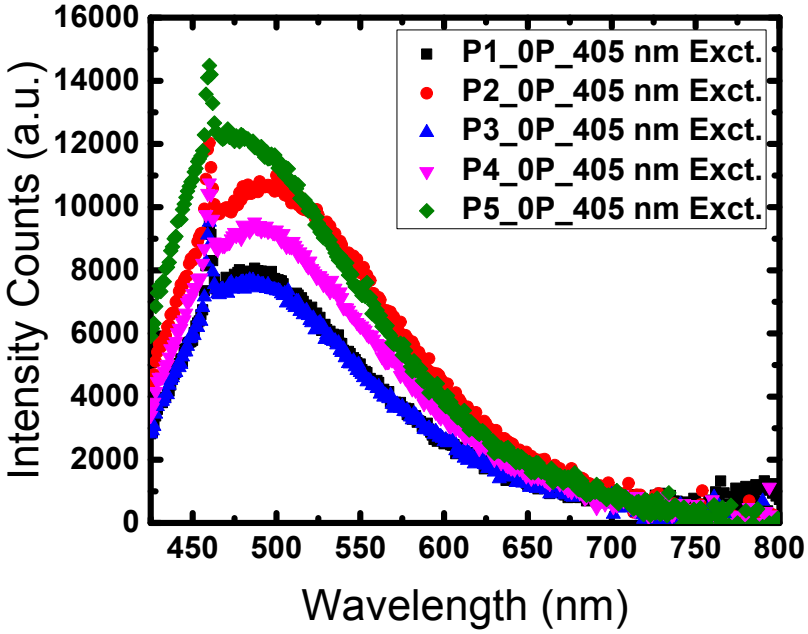

Figure S44: Emission Scan (PL) at 405 nm Excitation for P1-P5 Samples (*fw*-0 %).

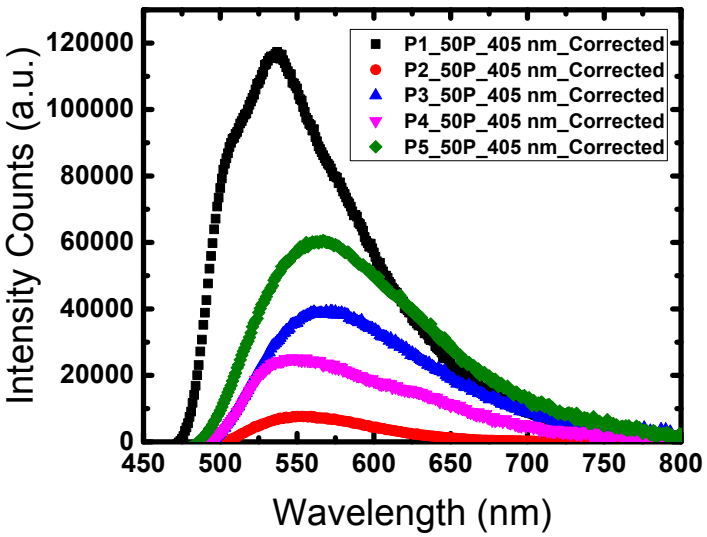

Figure S45: Emission Scan (PL) at 405 nm Excitation for P1-P5 (*fw*-50%) -Corrected for **DMSO.**

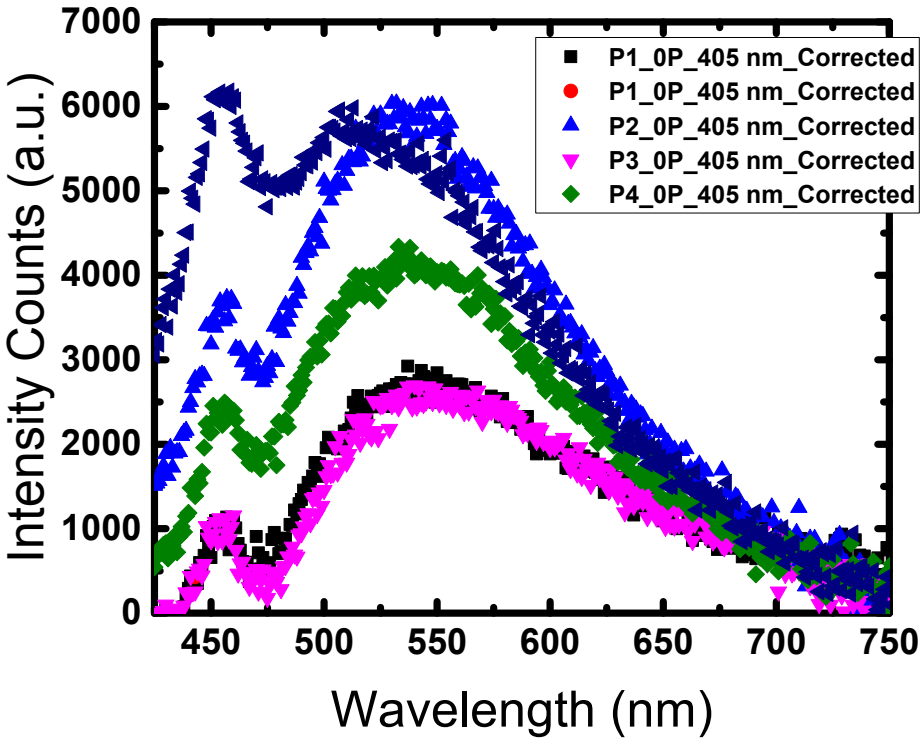

Figure S46: Emission Scan (PL) at 405 nm Excitation for P1-P5 (*fw*-0%) -Corrected for **DMSO.**

11.4 Comparing PL intensities (DMSO: Water)

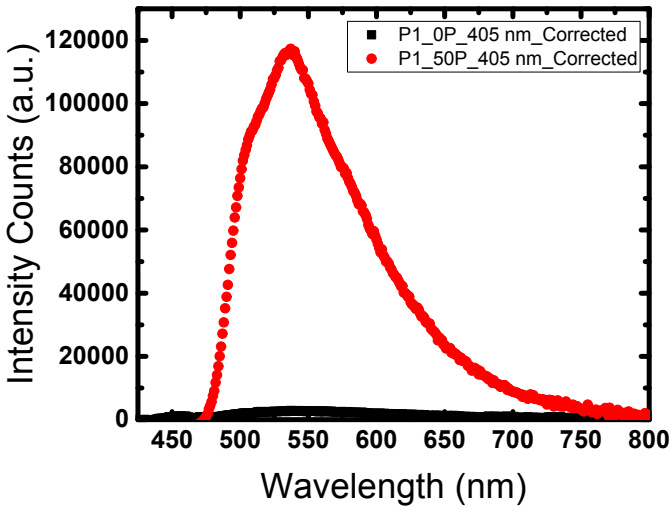

Figure S47: Comparison of PL intensities between *fw*-0-50% (DMSO: Water) for Luminogen **P-1.**

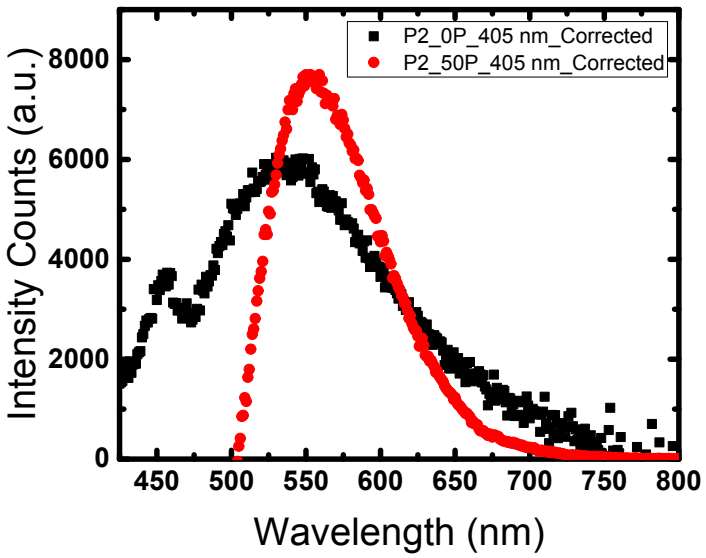

Figure S48: Comparison of PL intensities between *fw*-0-50% (DMSO: Water) for Luminogen **P-2.**

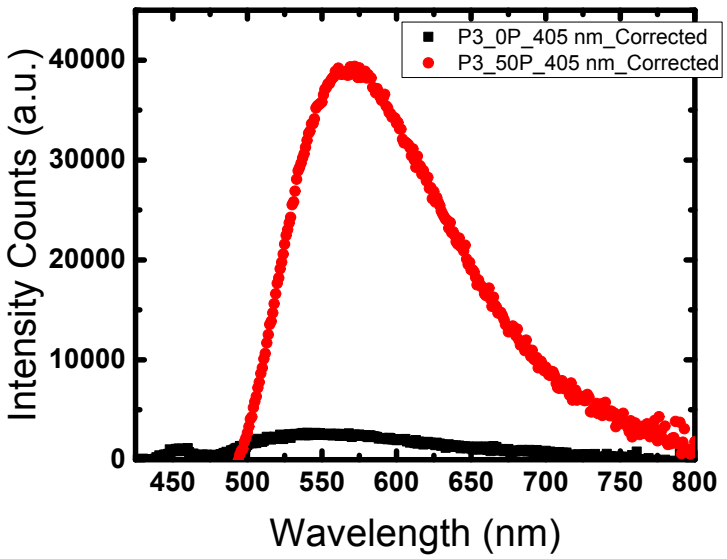

Figure S49: Comparison of PL intensities between *fw*-0-50% (DMSO: Water) for Luminogen **P-3.**

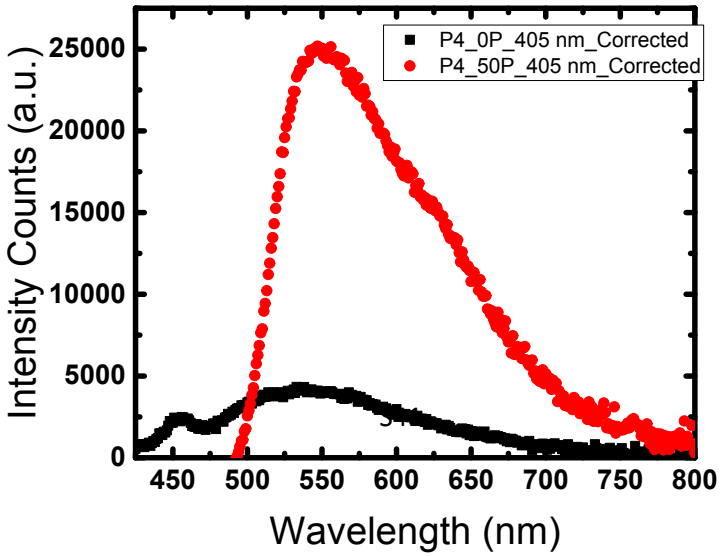

Figure S50: Comparison of PL intensities between *fw*-0-50% (DMSO: Water) for Luminogen **P-4.**

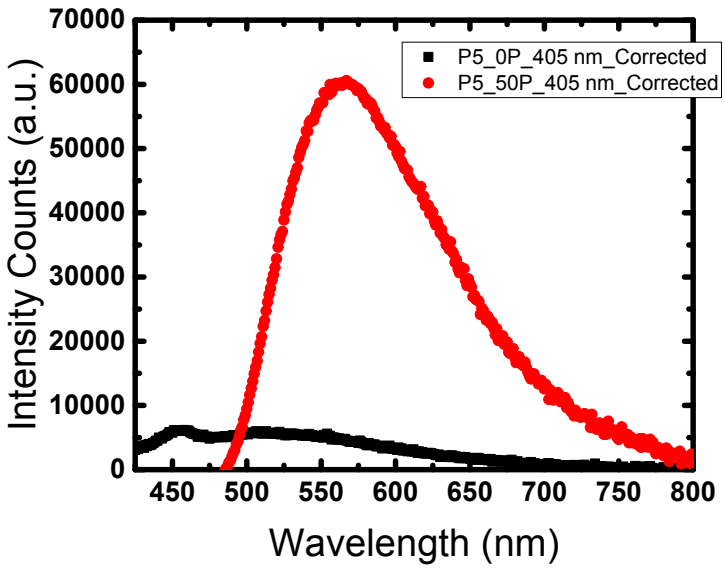

Figure S51: Comparison of PL intensities between *fw*-0-50% (DMSO: Water) for Luminogen **P-5.**

11.5 Quantum Yield Measurement for Solution state (Integrating Sphere Method)

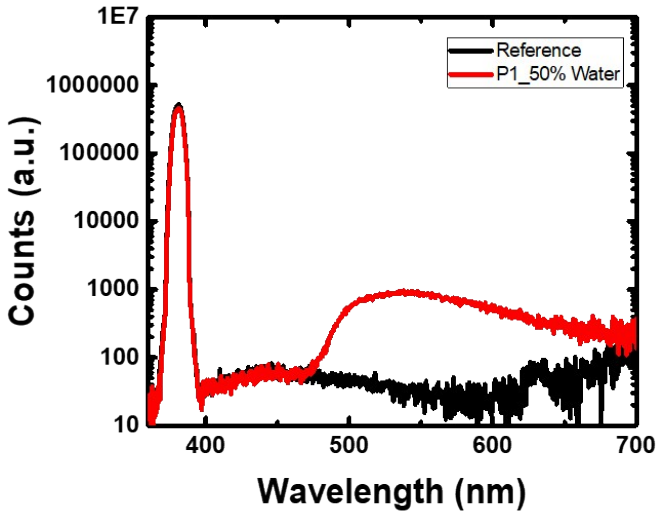

Scatter Range: 360.40 to 399.20 nm
Emission Range: 466.00 to 729.60 nm
Quantum yield (QY) = 19.92%

Figure S52: Quantum Yield for luminogen P1-*fw* 50% with DMSO and Water.

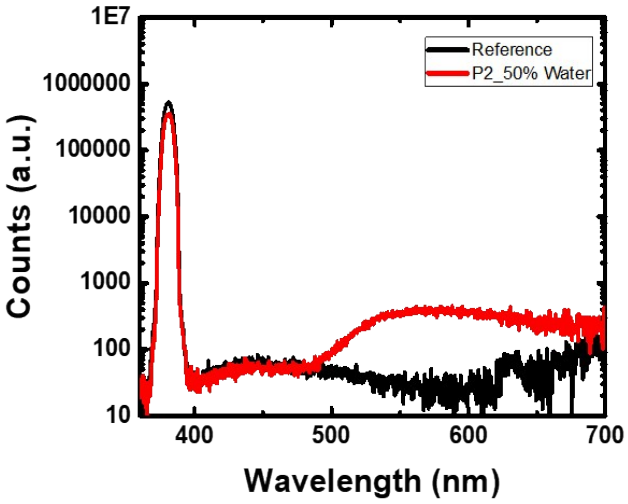

Scatter Range: 365.60 to 395.60 nm
Emission Range: 475.20 to 712.40 nm
Quantum yield (QY) = 3.69%

Figure S55: Quantum Yield for luminogen P2-*fw* 50% with DMSO and Water.

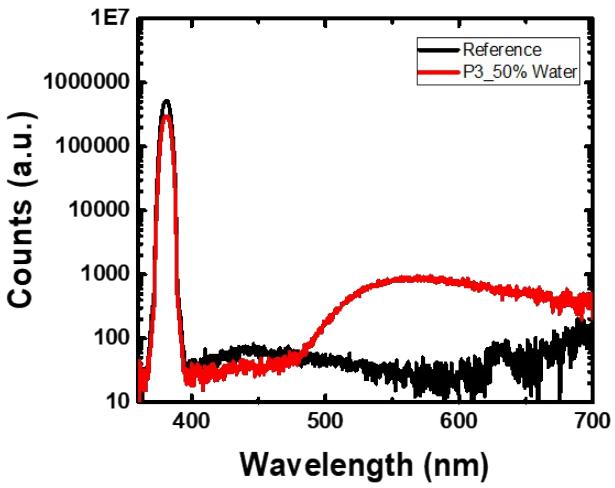

Scatter Range: 364.40 to 398.00 nm
Emission Range: 478.40 to 727.60 nm
Quantum yield (QY) = 6.56%

Figure S56: Quantum Yield for luminogen P3-*fw* 50% with DMSO and Water.

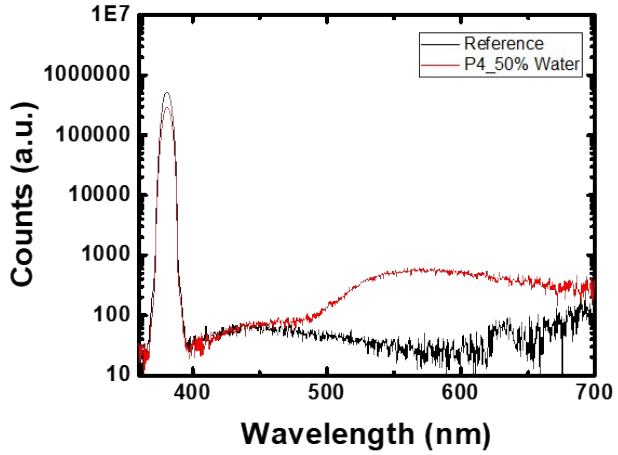

Scatter Range: 365.20 to 396.80 nm
Emission Range: 441.20 to 720.00 nm
Quantum yield (QY) = 4.06%

Figure S57: Quantum Yield for luminogen P4-*fw* 50% with DMSO and Water.

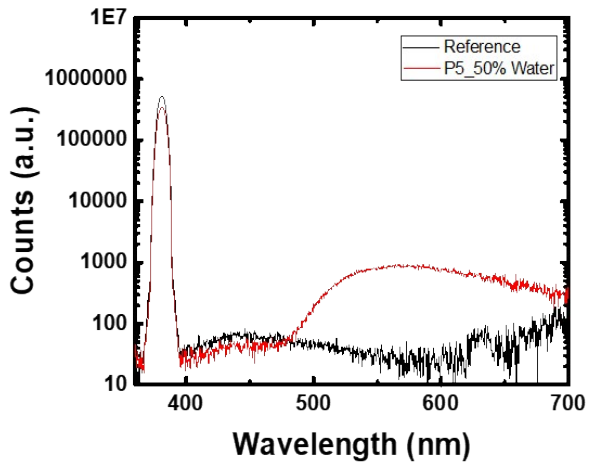

Scatter Range: 363.20 to 477.60 nm
Emission Range: 479.20 to 734.00 nm
Quantum yield (QY) = 8.17%

Figure S58: Quantum Yield for luminogen P5-*fw* 50% with DMSO and Water.

11.6 Tail Fitting of Time Resolved Decay (Solid Thin Film Samples)

	Fix	Value / ns	Std. Dev / ns		Fix	Value	Std. Dev	Rel %
τ_1	☐	12.3436	0.44289	B_1	☐	8359.983	1329.4503	77.02
τ_2	☐	17.5337	2.00149	B_2	☐	1755.780	1343.0774	22.98
τ_3	☐			B_3	☐			
τ_4	☐			B_4	☐			
				A	☐	31.125		

χ^2 : 1.131

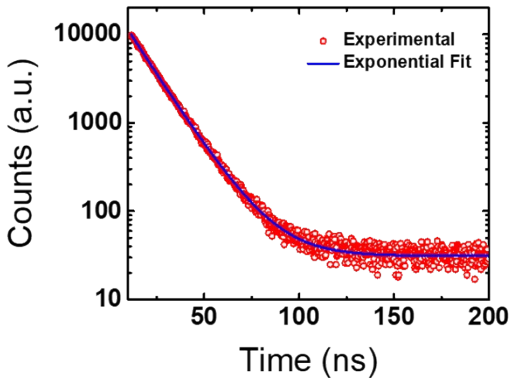

Figure S59: Lifetime studies of the Luminogen **P1.**

	Fix	Value / ns	Std. Dev / ns		Fix	Value	Std. Dev	Rel %
τ_1	☐	2.6721	0.04550	B_1	☐	7387.502	120.2823	56.13
τ_2	☐	6.3119	0.10257	B_2	☐	2444.500	135.1797	43.87
τ_3	☐			B_3	☐			
τ_4	☐			B_4	☐			
				A	☐	8.268		

χ^2 : 1.238

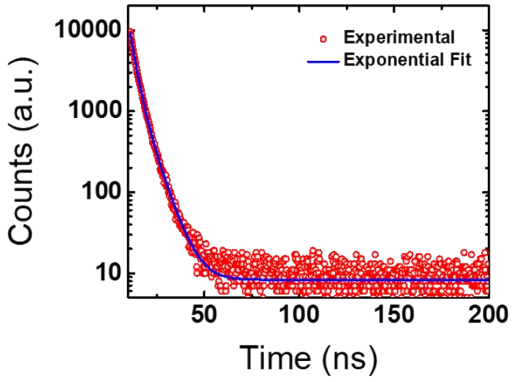

Figure S60: Lifetime studies of the Luminogen **P2.**

	Fix	Value / ns	Std. Dev / ns		Fix	Value	Std. Dev	Rel %
τ_1	☐	5.7666	0.16509	B_1	☐	6753.761	467.1703	53.89
τ_2	☐	9.7008	0.27417	B_2	☐	3435.671	484.8202	46.11
τ_3	☐			B_3	☐			
τ_4	☐			B_4	☐			
				A	☐	16.265		

χ^2 : 1.048

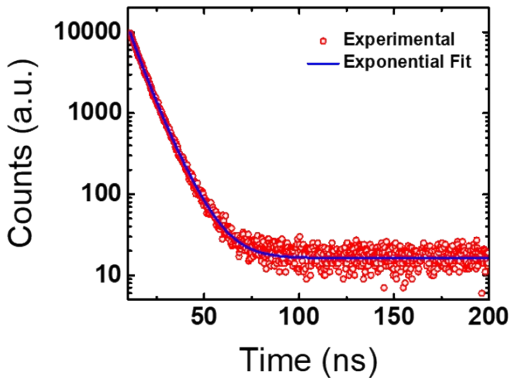

Figure S61: Lifetime studies of the Luminogen **P3.**

	Fix	Value / ns	Std. Dev / ns		Fix	Value	Std. Dev	Rel %
τ_1	☐	4.9435	0.12175	B_1	☐	6463.563	283.2412	47.82
τ_2	☐	9.2588	0.17232	B_2	☐	3765.012	300.6876	52.18
τ_3	☐			B_3	☐			
τ_4	☐			B_4	☐			
				A	☐	15.093		

χ^2 : 1.134

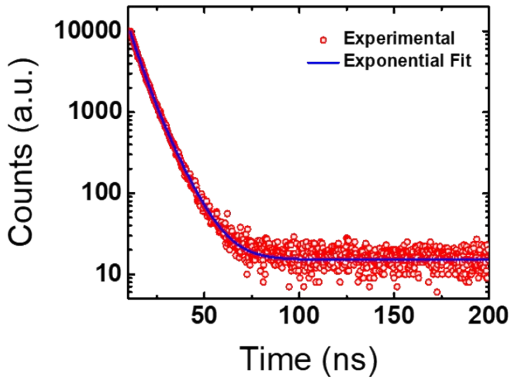

Figure S62: Lifetime studies of the Luminogen **P4.**

	Fix	Value / ns	Std. Dev / ns		Fix	Value	Std. Dev	Rel %
τ_1	☐	8.9311	0.07268	B_1	☐	10277.911	121.6276	96.72
τ_2	☐	18.0085	3.48805	B_2	☐	172.940	132.7223	3.28
τ_3	☐			B_3	☐			
τ_4	☐			B_4	☐			
				A	☐	17.083		

χ^2 : 1.277

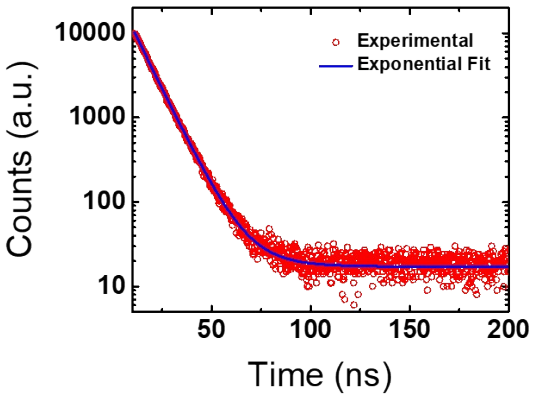

Figure S63: Lifetime studies of the Luminogen **P5.**